L621.3051
A438

ALLIS-CHALMERS Electrical REVIEW

4TH QUARTER 1959

THE JOHN CRERAR LIBRARY
JAN 14 1960

25 R 9505

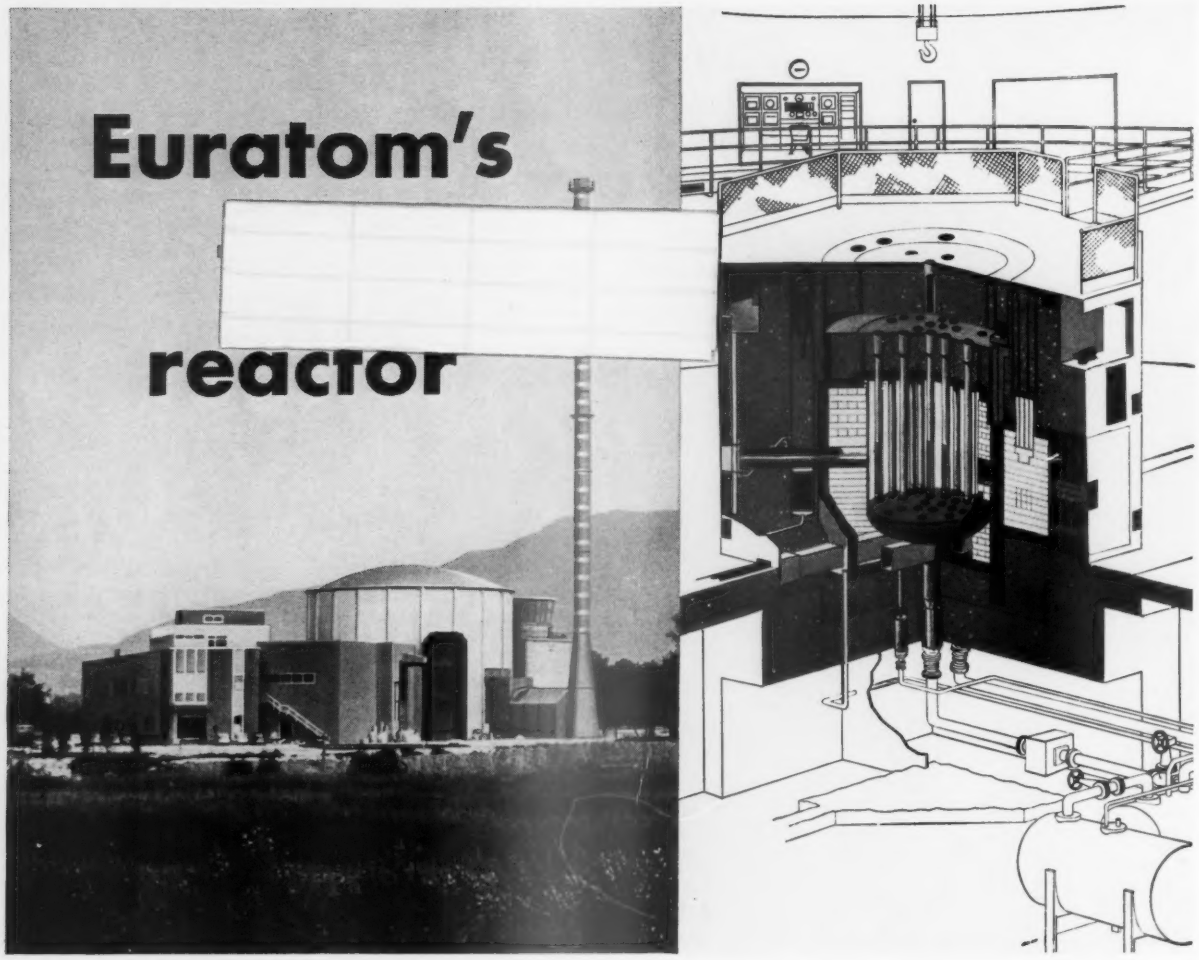

Designed and built by Allis-Chalmers, CNRN puts atoms to work for peace

Euratom's acquisition of the heavy-water research reactor designed and built by Allis-Chalmers for Italy's Comitato Nazionale per le Ricerche Nucleari is the first step in a billion-dollar, ten-year program designed to speed the development of nuclear power in Europe. This facility demonstrates the far-reaching abilities of Allis-Chalmers in the nuclear reactor field.

Located near Ispra, Italy, this 5000-kw reactor is now leased to Euratom and represents an important step ahead in the development of Atoms for Peace.

Noteworthy features of the CNRN reactor include 20% enriched fuel . . . dual-loop cooling system which permits operation at half power with one loop while the other is being serviced . . . facilities for isotope production.

Allis-Chalmers was also responsible for technical supervision during construction, installation, pre-operational testing and start-up. The contract was initiated in October of 1956, and the reactor went critical in March of 1959.

The CNRN reactor is another example of Allis-Chalmers unmatched capabilities and resources in the nuclear field. Whether your own plans are at the "talk-about" stage or ready for blueprints and estimates, you should get better acquainted with what Allis-Chalmers can offer. *A new brochure gives complete details. Write Allis-Chalmers, Atomic Energy Division, Milwaukee 1, Wisconsin.*

OTHER ALLIS-CHALMERS REACTOR PROJECTS INCLUDE: **MIT research reactor · Test and research reactors for Sweden and the Netherlands · Radiation effects reactor for USAF · Elk River and Pathfinder boiling water power reactors · experimental gas-cooled reactor for AEC.**

ALLIS-CHALMERS

A-1207

ALLIS-CHALMERS
Electrical REVIEW

THE COVER

ANSWERING PROCESS PROBLEMS for mining, metals and chemical industries, a new pilot plant at Carrollville, Wisconsin, was built to obtain new engineering information relating to a wide range of materials. Preparation of green balls, an important step in the Grate-Kiln system, can start from either dry or wet raw materials. The 39-inch balling pan shown is a laboratory size unit.

The plant, an actual miniature operating process plant about 1/40 the size of a full-scale plant, is described in the article on page 12, "Gathering Process Data."

Allis-Chalmers Staff Photo by J. E. Gosseck

Allis-Chalmers
ELECTRICAL REVIEW

Vol. XXIV No. 4

Executive Board
C. W. Schweers *F. W. Bush*
A. R. Tofte

Editor.....*R. W. Smeaton*
Managing Editor.....*G. R. Powers*
Technical Consultant.....*L. J. Linde*

Associate Editors
Boston Works.....*I. C. Fisk*
C-Stellarator.....*R. C. Dancy*
Control.....*R. W. Fugill*
Electrical Application.....*T. E. Bryan*
Heat Transfer & Water Conditioning *J. S. Ferguson*
Hydraulic.....*Edward Uehling*
Motor & Generator.....*F. C. Osterland*
Nuclear Power (Greendale Lab.)..... *Gunnar Johnson*
Nuclear Power (Washington, D. C.).. *R. W. Durante*
Office of Dir. of Engin.....*Robert Mudd*
Patent.....*H. L. Swenson*
Pittsburgh Works.....*F. J. McGaughey*
Plant Engineering.....*H. Mickowski*
Rectifier.....*A. E. Brown*
Regulator.....*Frank Ladd*
Research.....*R. F. Anderson*
Steam Turbine (Turbine)..... *M. C. Maloney*
Steam Turbine (Generator)..... *J. A. Zimmerman*
Switchgear.....*J. A. Keymar*
Terre Haute.....*B. A. Storaasli*
Transformer.....*L. W. Schoenig*

Layout Art Editor.....*S. M. Loch*
Production.....*J. E. Steffek*
Circulation.....*John Gumtz*

Issued quarterly. Subscription rates: U. S., Mexico, and Canada, $2.00 per year; other countries, $3.00; single copies, $1.00 in advance.

CONTENTS

Heavy-Duty Power . . . an evaluation of silicon rectifiers..... 4
Paul Triplett

Advances in Sealed Mercury-Arc Rectifiers..... 8
Charles Sturtzen

Gathering Process Data..... 12
Glenn M. Hansen

Balancing Thrust in Separate Turbine Elements..... 16
C. D. Wilson

Single Phasing Three-Phase Motors..... 20
R. C. Moore

Determining Thermal Transients..... 25
W. O. Vebber and T. R. Herman

Solving Multi-Winding Transformer Circuit Problems 30
A. H. Knable

Research & Development Provides Data for Advanced Nuclear Power Plant..... 36
D. H. Swanson

Indexed regularly by Engineering Index, Inc.
Allis-Chalmers ELECTRICAL REVIEW is available to public and institutional libraries on microfilm from University Microfilms, 313 N. First St., Ann Arbor, Mich.

Address Allis-Chalmers Electrical Review, Milwaukee 1, Wisconsin

Printed in U. S. A. Copyright 1960 by Allis-Chalmers Mfg. Co.

HEAVY-DUTY POWER

. . . an evaluation of silicon rectifiers

by **PAUL TRIPLETT**
Electrical Application Dept.
Allis-Chalmers Mfg. Co.

Silicon rectifiers are being widely used in general applications and modernization programs. Here are the reasons for their acceptance.

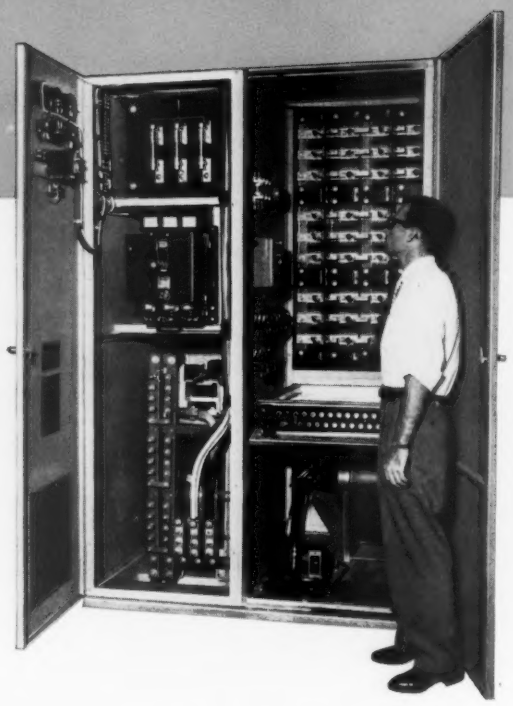

SILICON RECTIFIER, rated 150 kw at 125/250 volts, powers elevators, lights and other essential building services. The diodes are installed in individual cast aluminum heat sinks. **(FIGURE 1)**

THE WIDESPREAD INCREASE in the use of constant potential dc power in industry has provided great impetus for the development of reliable conversion equipment.

The advent of the silicon power diode about five years ago made possible the development of the silicon rectifier for heavy-duty industrial use. Installations like the one shown in Figure 1 are typical.

Rectifiers are proved to be reliable

Reliability is always relative. Batteries when adequately maintained have historically been considered the most reliable source of dc power, but their cost for large commercial and industrial applications has always been prohibitive. Even when batteries are considered necessary as stand-by equipment, the high capital investment usually limits their use to emergency operation.

For economic reasons lower-cost rotating machines were the first conversion units developed to deliver large blocks of dc power. The dc generator has a significant advantage, since it can be driven by a variety of prime movers. In the past, when the utmost in reliability was required, powerhouses were often built to obtain complete system control.

As ac distribution systems approached their present dependability, induction or synchronous motors were used for dc generator drives. Rotary converters were satisfactorily used in areas where output voltage stabilization was unimportant. They had the advantage of combining the motor and generator functions in a single unit. Until mercury-arc rectifiers appeared, motor-generator sets accounted for most of the dc conversion equipment.

Even though rectifiers were mistrusted by many engineers when first introduced, the advantages of static devices could not be overlooked. Then as now, rectifiers are lower in installed cost per kw, are more efficient and require far less maintenance than do rotating combinations.

Large-scale use of power rectifiers began on street railway, subway and rapid transit systems. Automatic controls were easy to add and enabled user substations to operate unattended. In railway service rectifiers were particularly advantageous because of their low idling losses and inherent ability to deliver large amounts of power on demand. Many early rectifiers were retired only when the electric transit vehicle began to disappear.

High efficiency with close voltage control and immunity to corrosive atmospheres are the predominant reasons for the acceptance of mercury-arc rectifiers by the electrochemical industry, because power cost often outweighs the cost of raw materials. High maintenance cost resulting from corrosion of commutators and brushes is common with rotary-type converters.

In industrial applications when highest operating efficiency is not the critical consideration, mercury-arc rectifiers are preferred because of other user advantages. For example, costly foundations and ventilating systems are unnecessary and an ability to operate unattended makes rectifiers most attractive for new plant systems.

Rectifiers are compared

The success of mercury-arc rectifiers for industrial duty has provided a smooth transition to the newer silicon type.

The mercury-arc versus silicon comparison is primarily a matter of degree and application. Both types have

characteristics that are desirable in given situations. Properly applied silicon diodes have unlimited life for reliable and continuous service compared to the slow, gradual aging of mercury-arc tubes. With mercury-arc tubes, however, voltage control is inherent. By requiring fewer auxiliary devices the silicon rectifier has correspondingly fewer maintenance items than mercury-arc rectifiers.

Testing guarantees quality

The silicon diodes are the heart of the silicon rectifier unit. Since there are as yet no industry standards available defining silicon cell performance, every effort must be made to insure that only the best silicon cells are used in a rectifier. A program of exhaustive testing by the manufacturers is necessary to determine the exact power rating and temperature characteristics of each diode. Operating and allowable overload conditions are investigated and units either "pass" or "fail." Only the silicon diodes that satisfactorily complete every test are installed in a rectifier.

Operating temperature is the critical consideration. To establish the most efficient and effective method to dissipate diode losses, tests of different cooling fin configurations are made. Facilities for measurement of air velocity, air and diode temperature have provided design engineers with the basic data to solve the cooling problem. Figure 2 shows the cooling fin optimum design.

As air pressure is a factor in determining air flow efficiency, the recording barometric pressure apparatus shown in Figure 3 is used by the design engineers.

Adequate protection is essential

Silicon diodes have virtually unlimited, trouble-free life when operated within their rating. They are, however, temperature sensitive because their mass is small and are subject to rapid temperature rise during overcurrents. If an excessive overcurrent were permitted for even a few seconds, a silicon diode would suddenly fail, but a correct choice of protective devices will prevent damage.

Prominent among the factors considered in the design of silicon rectifiers are the continuous and overload current ratings, the short-time current-carrying capacity of the silicon diodes with respect to the magnitude of the available short-circuit current, and the speed with which the protective circuit breaker interrupts this fault current. Frequently a design solution indicates that breaker speed is the deciding factor in determining the number of diodes that should be used in a unit. A high speed circuit breaker will often permit the achievement of a sound, coordinated design without resorting to an excessive number of diodes because of short-circuit considerations.

BAROMETRIC PRESSURE is a factor in determining the air flow across diodes. The pressure drop across the diodes is calibrated to obtain the actual air flow. These measurements, combined with diode and air temperature at various loads, provide data to determine the optimum cooling for conservative application. **(FIGURE 3)**

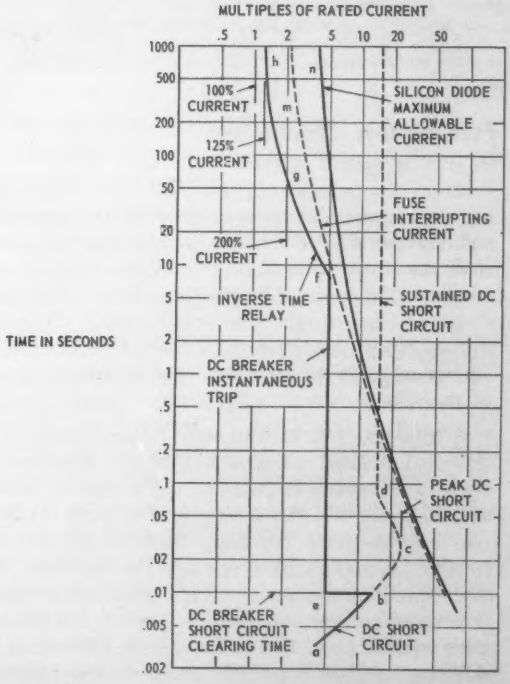

COORDINATION CURVES show the rectifier diode protective system. Point c is at about 25 times the rectifier rating and operation at point g permits 200 percent current for one minute. **(FIGURE 4)**

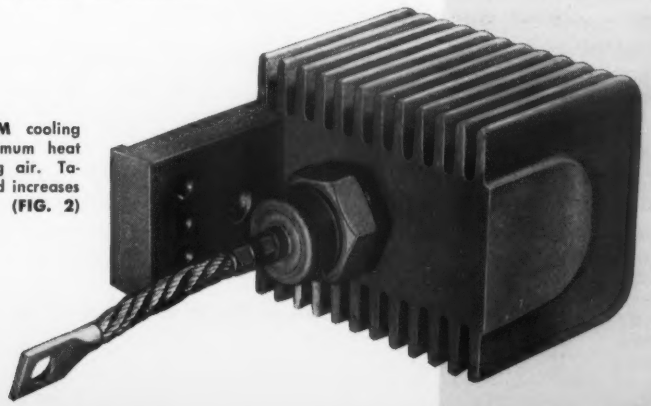

CAST ALUMINUM cooling fins provide maximum heat transfer to cooling air. Tapered diode thread increases thermal capacity. **(FIG. 2)**

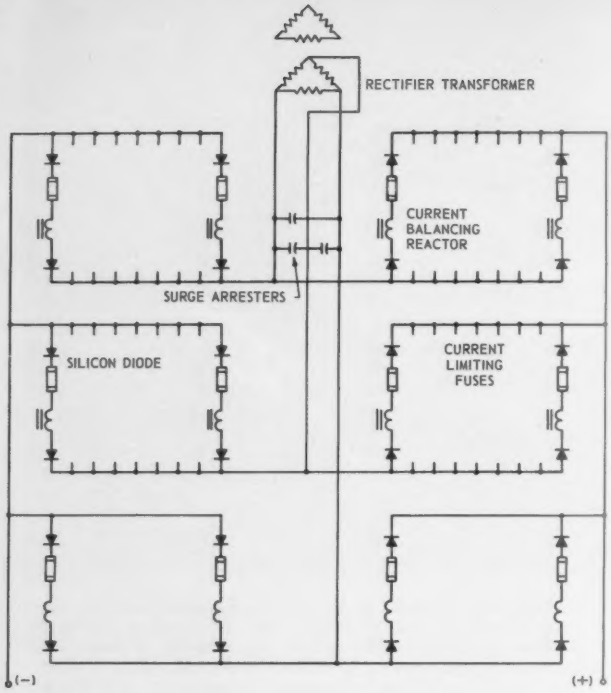

DOUBLE-WAY CIRCUIT includes nine parallel rectifier diodes in each phase. Each element consists of two diodes, a current balancing reactor and a current-limiting fuse in series. **(FIGURE 5)**

Fast breaker clears faults

Protection against external faults is the most important function of a protective system. Even though an installation is designed and operated correctly, fault currents can and do occur. Curve *abcd* in Figure 4 is the direct current from the worst external fault condition, which is a short circuit on the dc load. Point *d* and above is the maximum sustained fault current that would exist if no protective devices operated. Above point *d* the heat from the fault current exists for a longer time than the thermal capability of the silicon diodes.

A high speed dc breaker with current-limiting characteristics will limit excessive fault current and prevent the opening of internal current-limiting silicon cell fuses. The actual current will rise no higher than point *b*, since the line *eb* represents the total interrupting time of the breaker. Circuit breaker selection is important because high speed operation can clear faults before maximum destructive currents are reached. Curve *fgh* is the inverse-time overload protection for the diodes. This characteristic is located as close as possible to the diode maximum current to permit dc feeder breakers to operate before the main ac breaker provides backup protection.

High speed fuses limit internal faults

Even though silicon diodes have seldom been known to fail, high speed current-limiting fuses, shown in Figure 5, will protect the remaining diodes if, for any reason, there should be a failure. Two units, connected in series, are protected by a common fuse. If a diode should fail and short out, fault current is supplied from the other two phases. The fuse must limit the fault current supplied from the other two phases on the same side of the bridge from exceeding the thermal capacity of the unfaulted diodes. In Figure 4 curve *m* represents the clearing time of the fuse in the faulted diode and curve *n* represents the thermal capacity of the unfaulted diodes. These characteristics insure that all internal faults are cleared without damage to the remaining diodes and without interruption of output power.

If for any reason a group of diodes should fail, it would be switched out of the circuit in 0.01 seconds; the remaining diodes in the phase have sufficient capacity to carry normal loads. Replacement of energized diodes is eliminated. Units are usually designed to shut down automatically if a second diode should fail in the same leg of the bridge in any phase, but operation can be resumed at reduced capacity.

Load division among paralleled diodes is closely controlled by balancing reactors. These reactors insure that load unbalance will never exceed 10 percent. Since rectifier diodes are rated to carry the 10 percent unbalance continuously, failures will not result from internal overloads.

Cooling methods provide flexibility

In the simplest type of air-cooling system ambient air is drawn directly into the rectifier unit where it cools the diodes and is then exhausted. The circulation of forced air across rectifier cooling fins will carry away accumulated heat, but increased cooling efficiency can be obtained by directing the air at fairly high pressure into a vertical plenum chamber. With rectifier diodes mounted across openings in the chamber, the air is forced across all the fins and cooling will be essentially the same for all diodes regardless of their position in the chamber. In many installations rectifier equipment is located in controlled atmospheres, such as those found in motor rooms, which makes the simple system entirely satisfactory. Air filters in the rectifier air intake provide additional control of air cleanliness.

When circumstances do not permit direct air cooling, a recirculating, forced-air cooling system with an air-to-water heat exchanger can be used. After the air has passed over the diode cooling fins, it goes through the air-to-water heat exchanger and is then recirculated to the plenum chamber. This scheme minimizes the effects of contaminated air and makes the cooling air temperature independent of the ambient air temperature. It is also possible to water-cool the diodes, either directly, or indirectly by using a heat exchanger.

Automatic devices protect equipment

A thermostat and an air flow switch will protect against high compartment temperatures and loss of air flow. A water flow switch can shut down the unit if cooling water fails to circulate through the heat exchanger.

Auxiliary protective systems are arranged to give indication of difficulty and can be made to shut down the unit. In usual situations where the load may not be

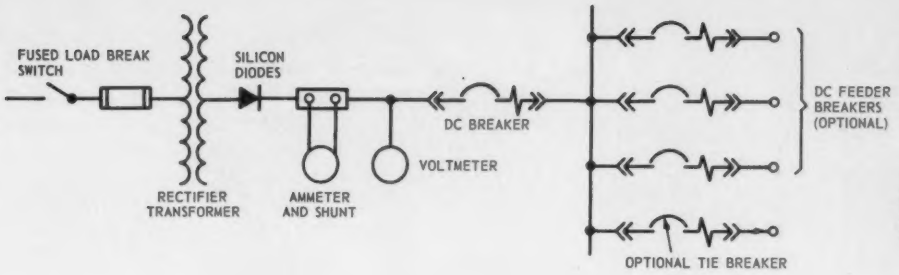

SINGLE-LINE diagram shows typical silicon rectifier circuit. Component flexibility permits several arrangements. **(FIG. 6)**

critical, the protective system will shut the unit down in case of malfunction. However, in critical situations a signal system will indicate a difficulty, but an operator has control of the shutdown.

In common with mercury-arc rectifiers, silicon units cannot handle reverse power flow. Reverse power can occur when the total load is light and a large crane or elevator is overhauling. Under this condition, a motor will act as a generator and attempt to feed power back into the rectifier. Since this is impossible, the bus voltage will rise, flash over motor commutators and, in extreme cases, the bus insulation as well.

Dynamic-braking resistors in the rectifier output circuit will limit voltage rise during periods of regenerating power. Automatically applying these resistors upon a rise in bus voltage until the reverse power flow stops will maintain the bus voltage at an acceptable level. Usually a resistor sized in kw at 40 to 50 percent of the largest motor in the system provides adequate braking capacity. Table I lists the resistors that can be used with typical rectifier capacities.

Rectifiers can be safely paralleled

Silicon rectifiers with their straight-line drooping voltage characteristic are well suited for parallel operation, either with additional silicon units or with mercury-arc rectifiers. Small units are advantageously operated in parallel instead of using a single large unit. A slight voltage drop (6 percent from no load to full load) forces proper load division even among units of different sizes.

If the output voltages of the machines to be paralleled do not match, load division regulators are required. This is particularly true if the paralleled machines are physically close together.

When a voltage mismatch occurs and the machines are widely separated, the cable impedance between the machines becomes an important factor in controlling load division. Load division regulators may or may not be required, depending on the location of the feeder circuit take-off points. An engineering evaluation is required for such situations.

When widely separated units fail to divide load properly, load balance equipment will compensate for the unbalanced voltage drop in the tie busses. Load balance regulators can often be eliminated if the sizing of tie cables and the selection of tap-off feeder points are carefully considered.

Paralleling with m-g sets, however, will usually require voltage regulators and load division equipment. The characteristics of the rotating machine must be known before paralleling requirements can be determined.

Rectifier is complete dc system

A complete heavy-duty silicon rectifier includes all necessary components in four units. These are:

1. Load-break switch and fuse combination, or circuit breaker.

2. Dry-type or liquid-filled transformer.

3. Air-cooled silicon diodes, cooling equipment and fuse-monitoring equipment.

4. Dc breaker, ammeter and shunt, voltmeter, operation counter, main control switch and indicating lights. The dc breaker is necessarily required in situations where an ac breaker is used. A diagram of the assembly is shown in Figure 6.

Table II lists standard sized units that can carry 100 percent load continuously, and loads of 125 percent current for two hours or 200 percent for one minute without harm to the unit. Full load can precede or follow the specified overloads. Standard supply voltages are 2400, 4160, 4800, 6900, 7200, 12,000, 13,200 and 13,800 volts, three phase, 60 cycles. A three-phase undervoltage relay will shut down the unit if a phase should open in the rectifier transformer primary circuit.

Rectifiers are static devices and not subject to the mechanical limitations usually associated with rotating combinations with their lubrication and maintenance problems. They operate unattended and are a dependable source of closely regulated dc power. Today, silicon rectifiers are being used in ever increasing numbers in a variety of industrial applications.

TABLE I

Rectifier Size Kw	Dynamic Braking Resistor Size Kw
400	30
500	40
600	50
750	60
1,000	80
1,500	80
2,000	80

TABLE II

Kw	100% Current	125% Current	200% Current
400	1,600	2,000	3,200
500	2,000	2,500	4,000
600	2,400	3,000	4,800
750	3,000	3,750	6,000
1,000	4,000	5,000	8,000
1,500	6,000	7,500	12,000
2,000	8,000	10,000	16,000

ADVANCES IN SEALED MERCURY-ARC RECTIFIERS

by **CHARLES STURTZEN**
Rectifier Section
Allis-Chalmers Mfg. Co.

SIX-TUBE DEAD-FRONT rectifier assembly is rated 1000 kw at 250 volts dc. Similar units are used in general industrial applications, including steel mill and electrochemical installations.

The sealed tube of today is the result of half a century of development and experience. New techniques improve vacuum and eliminate separate forming operation.

STARTING AS A LABORATORY experiment, the sealed mercury-arc rectifier is now a high-capacity industrial unit. Continuous power levels of 500 amperes at 600 to 700 volts per tube are coupled with efficient, trouble-free and static operation. Current capacity of up to 800 amperes is available at lower voltage.

Practically all early tubes were made of glass and had small current capacities. Figure 1 shows a glass multi-element tube in operation, but early experience indicated that the development of steel tanks with multiple-anode arrangement would be desirable. The steel tank required insulation between the anode inlets, the steel envelope, and the cathode. A tank with a demountable cover plate was used in initial developments because of frequent, necessary overhauling.

Design solutions furthered development

In common with low power vacuum tubes a high vacuum is essential to limit the conduction phenomena in mercury-arc rectifiers to a controlled mercury ionization. Most problems, such as maintaining high vacuum, the construction of various types of pumps, hermetic sealing, and efficient production, found practical solutions during the first twenty years of tube application. Attention was concentrated on improving the operation of rectifiers and increasing their load-carrying capacity. Steel anodes were replaced by anodes of graphite, while rubber gaskets displaced asbestos. Figure 2 shows a line-up of multi-element tubes; the tube in Figure 3 is air cooled.

At the end of the twenties, the first grid-controlled rectifiers entered the market. Departure from the multi-anode types began soon after. An early tube design is shown in Figure 4. The trend toward single-anode tubes was prompted by the desire for standardization, production control, exchange flexibility and, not least, by the advantage of a lower arc drop with an increased load per anode. Single-anode units with continuous holding arc and others with periodic ignition were developed.

Gas-free metals are required

As the mercury-arc rectifier came of age, its field of application steadily widened. No longer was its application limited to supplying direct-current networks, but it became equally useful in converting direct current into alternating current as well as changing alternating current of one frequency into alternating current of a different frequency.

The high power tube had become a versatile instrument. The assembling of vacuum seals no longer required trained experts. Improved materials, free of flaws and porosities, together with progress in welding techniques, produced tubes with negligible air seepage.

A perfectly tight high power rectifier was a logical consideration. Sealing off was easy, since every rectifier was equipped with a vacuum valve and experiments were relatively successful. It was possible to run units without vacuum pumps from one day to one week. Although this was far from the ultimate goal of a permanently sealed tube capable of maintaining a high vacuum over many years of service, the experiments brought to light that the vacuum could be maintained only if it were possible to eliminate gas evolution from the rectifier materials. This problem could be tackled in two ways:

1) Using only materials with little or no gas content.
2) Eliminating the gas content of the material by a pretreatment.

Improved metallurgy solves problem

Of all known materials, none is free of gas and many vaporize continuously. Practically all organic substances are in this group. Although rubber proved to be a most convenient sealing medium, it is not now used in sealed-off rectifiers. In addition to choosing materials with lowest gas pressure, it became increasingly necessary to improve degassing processes.

Raising the temperature of the rectifier tube to drive out occluded gases is called rectifier forming. Thirty years ago the vacuum envelope was heated by circulating hot water through the cooling jackets and heating the tube interior by an electric arc between anode and cathode. The process started with a low anode current, which was gradually increased, depending on the rate of gas evolution — gas pressure was measured by a Pirani gauge. When the anode current reached a value corresponding to the tube's maximum rating or some set value above it, forming continued until the rate of gas evolution had diminished to a level at which the pumps could maintain the necessary vacuum for safe rectifier operation at rated voltage.

To avoid arc-backs or undesirable secondary arcs during forming, a low voltage source was used and predetermined vacuum limits were held. Forming is a slow procedure, unless the materials have previously undergone degassing.

From 1930 until the outbreak of the second world war, much new knowledge was acquired about the nature of gas evolution from steel at various temperatures and the way these gases become re-absorbed in the graphite and the steel parts of a rectifier during operation.

Early processing was time consuming

A temperature of 400 C was found sufficiently high for adequate degassing of the container. Because rectifier anodes operate at temperatures much higher than 400 C, tubes were degassed in a furnace by heating to 400 C followed by current forming of the anode at reduced tank temperature. This required alternate removal of mercury from the tank during the 400 C baking and redistilling of mercury into the tank for anode current forming. Rectifier processing by this procedure was cumbersome and time consuming. But tubes could be sealed off and their vacuum maintained for many months, even years, if no seepage occurred through the envelope. During operation sealed-off rectifiers were cooled almost exclusively by forced air, since water cooling was not suitable.

Tests showed that sealed units with water cooling became inoperative after a short time because of the presence of monatomic hydrogen in the cooling water. This hydrogen diffuses easily along the grain boundaries of the steel into the rectifier, where it accumulates, recombines to molecules, and impairs the vacuum. Under the influence of an electric arc the hydrogen becomes ionized and disappears in the surrounding steel parts after a short time. Hydrogen diffusion through the tank wall is proportional to its concentration in the cooling water. This diffusion is accelerated by surface corrosion and temperature.

While water treated with sodium chromate can reduce the creation of free hydrogen to less than one percent of what normally prevails in uninhibited water, the reduction is insufficient for a permanently sealed tube.

GLASS envelopes were used in the first mercury-arc power rectifiers. Six-anode tube shown was rated at 250 volts and 400 amps. **(FIG. 1)**

Metallurgical research with ferrous alloys developed stainless steels whose surface remains corrosion resistant, and thus prevents the creation of monatomic hydrogen at its surface. The proper type of stainless steel, sufficiently stabilized, will prevent carbide precipitation at its grain boundaries even when kept for a considerable length of time at critical temperatures. This property is of extreme importance, since it made possible an entirely new approach to degassing rectifier tubes.

Extended areas are explored

Can sealed tubes be degassed in a single operation without current-forming the anodes? The fully assembled rectifier must be heated to about 900 C, far above the maximum service temperature of the main anode, and the rectifier has to endure this heat during the degassing process.

NEARLY 25 YEARS AGO these rectifiers were the largest installation in the country, over 54,000 kw. Anodes were water cooled. **(FIG. 2)**

EARLY TUBES were either air or water cooled. Tube shown has fan directing air up through the housing around tube. **(FIG. 3)**

HIGH VOLTAGE tube included high vacuum pump and a solenoid-operated ignition rod. Dome provides added cooling. **(FIG. 4)**

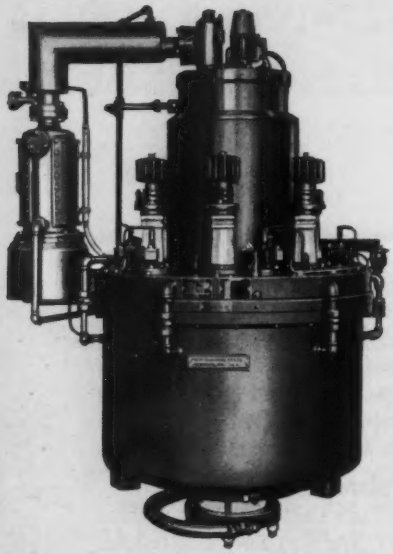

NEWEST sealed tube is shown being lowered into furnace. When the desired vacuum is reached and mercury is admitted through the vacuum line, the formed mercury vapor condenses in the water-cooled vacuum line. Mercury reservoir and release valve are above the vacuum connection. **(FIGURE 5)**

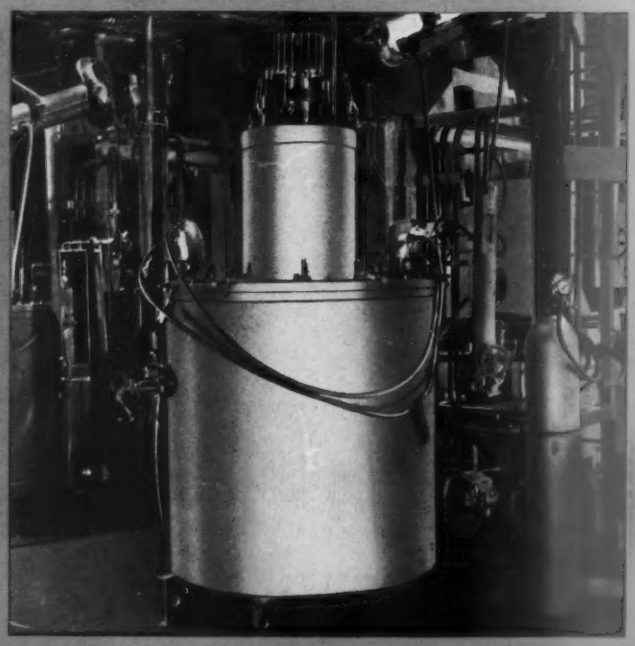

Tubes will withstand the necessary heating, except for the current inlets above the anode plate. The inlets consist of enameled members fused together to form an electrically insulated, vacuum-tight seal. Fortunately, because of their high thermal stability, these parts can easily stand a degassing temperature of 450 C, but the necessary temperature for the anodes is 900 C. Heat must be applied at 900 C below the anode plate and at 450 C above the plate.

The process must be performed under vacuum because a rectifier tube at 900 C could not stand the load of atmospheric pressure and the presence of air would oxydize it excessively. Furthermore, compactness and simplicity are desirable if users who wish to do their own tube reprocessing were to acquire such equipment.

Process method is greatly simplified

Present techniques have met the necessary requirements for continuous and reliable sealed-tube operation. With the different sizes of vacuum furnaces available, all rectifier tubes, from the smallest to the largest, can be processed.

Figure 5 shows the main body of one of the larger furnaces into which an 800-amp rectifier is being lowered. The rectifier is lowered until its anode plate is at the height of the furnace cover plate and remains suspended in this location. Figure 6 shows the final position of the rectifier with the water-cooled dome being guided over the rectifier vacuum line.

The vacuum line is concealed by the split water jackets clamped against it, as shown in Figure 7. Just above the vertical vacuum line is a rectangular release valve. The valve permits a controlled flow of mercury from a reservoir that contains the exact amount of mercury the rectifier is to receive at the end of bake-out.

All these devices are evacuated simultaneously through the high vacuum line connected to a diffusion pump backed by a mechanical roughing pump. The furnace is evacuated by a separate pump unit. The capacities of the various evacuating equipment are matched to the size of the furnace and rectifier tube so that all pumps can begin operating at the same time. When the rectifier reaches a vacuum of one micron or better, heater current is switched on and cooling water begins circulating.

Radiant heater elements surround the rectifier tank over the full length, from foot of tube to anode plate. Within a few hours the entire structure between foot and anode plate is heated to 900 C. To reduce heat loss to the furnace envelope, radiation shields are arranged between the heating elements and furnace wall in a radial as well as axial direction. Enough elements have been chosen to limit heat losses to an acceptable value.

The power input is exactly balanced with the desired furnace temperature and needs no adjustment. Once switched on, the furnace can be left unattended to the end of bake-out. Only when the vacuum in the rectifier or in the furnace drops excessively is the power switched off automatically and kept off until the vacuum recovers. A low vacuum is not critical, since the degassing occurs without voltage, free of any internal discharge phenomena as happens during current forming.

At the end of 24 to 30 hours of baking, the gas evolution approaches an insignificant rate. Heating is now

terminated; the furnace cools down. When the rectifier reaches a dull red heat, the mercury release valve is opened, permitting mercury to trickle slowly into the hot tube below, where it immediately vaporizes. The vapor builds up to a fairly high pressure, shooting upward through the vacuum line into the main high vacuum line where it condenses, and then returns to the rectifier.

Only one manual operation is required

During the bake cycle all gases in the mercury become liberated and pumped away to the atmosphere. Only during this time is it necessary to cool the pipe connection between dome and upper seal. Half an hour is sufficient to transfer all mercury to the rectifier and degas it by redistillation. The opening of the mercury release valve is the only manual operation after closing the main switch. A permanent graph is obtained of the rectifier wall temperature by thermocouple and recording instrument.

Before the furnace is back to room temperature, helium is permitted into its interior. A helium-sensitive leak detector switched into the rectifier vacuum connection indicates promptly any possible seepage. If the rectifier proves to be vacuum tight, it is ready for the next operation — the sealing off. The leak detection also helps to cool the furnace to a point where it is safe to admit air. When atmospheric pressure is reached inside the furnace, the seal between dome and vacuum line is loosened, the clamps are disengaged, and the dome is raised and set on supporting blocks, as shown in Figure 8. A low voltage transformer supplies current through the lower part of the vacuum line, heating the pipe up to white heat. Any further gas evolved in consequence is quickly drawn away. In less than a minute the vacuum line is forge-welded, forming a permanently tight seal. After the pinched section is cut through, the rectifier is ready for removal from the furnace.

Vacuum improves during operation

Operating experience proved that satisfactory vacuum was maintained even though sealed tubes had been stored for two years and more before being placed in service. During experiments when some gases were purposely admitted, even in cases where gas pressure had lowered the vacuum appreciably, it was possible to re-establish a high vacuum by starting an arc in the rectifier. The highly degassed graphite and steel display strong getter action. Oxygen as well as water vapor are eagerly taken up by the iron even without an ionizing arc. Nitrogen and hydrogen require an arc. Oxygen and nitrogen will become chemically bound with the iron and thus disappear permanently as gases. Rectifiers that have undergone this present treatment were found to improve their vacuum steadily during operation.

The sealed-tube rectifier produces dependable power at competitive cost. The tube is not just an enlarged version of the small, glass-envelope mercury tube, but is carefully developed for high level current conduction and designed to produce dc power required by basic industries.

Of the several types of dc power units available, the sealed mercury-arc tube is well suited for applications where voltage control is required and maintenance-free operation is assured.

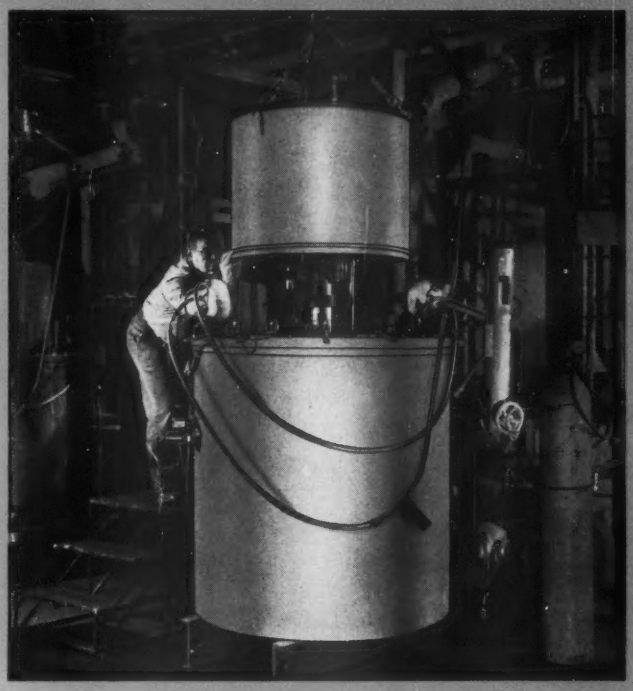

FURNACE DOME is shown being lowered over rectifier tube in the furnace prior to degassing. McLeod gauge at right checks vacuum. **(FIG. 6)**

VACUUM CONNECTION is sealed after the furnace dome is clamped to furnace tank. Tube vacuum line is held in a water jacket. **(FIG. 7)**

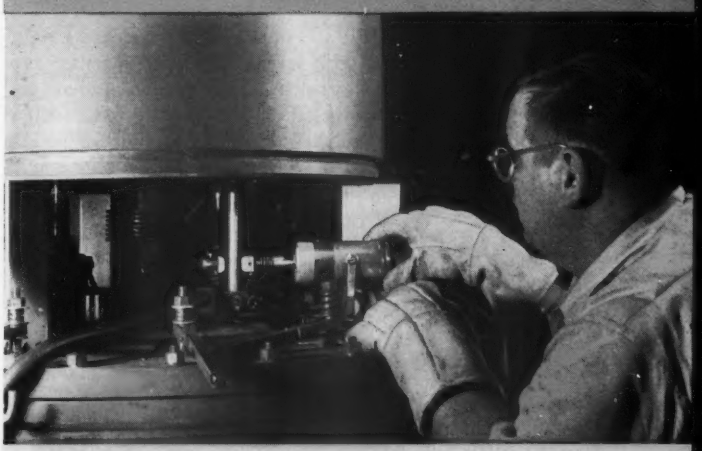

WHITE HOT vacuum line is forge welded by a specially designed pneumatic hammer. This operation completes the degassing process. **(FIG. 8)**

NERVE CENTER of pilot plant is the master control panel from which the overall operations are coordinated. Data gathered on recorders and indicators for air flow, temperature, and pressure provide engineers with the information needed to design plants for new processes.

GATHERING PROCESS DATA

by **GLENN M. HANSEN**
Processing Machinery Dept.
Allis-Chalmers Mfg. Co.

Accelerated developments in the process industry promise to relieve shortages of certain basic raw materials.

DWINDLING SUPPLIES of high-grade ores and mounting operating costs have spurred the need for new process techniques. Furthermore, greater attention to air pollution problems is bringing about new equipment designs for control of dust and gaseous waste being dissipated into the atmosphere.

Since process plant designs are dependent on accurate and dependable data obtained from actual operating experience, a new pilot plant was built, based on an advanced concept of a traveling grate-rotary kiln system.

The new plant was designed and constructed to answer numerous process questions relating to a diversity of raw materials. Finely ground hematite and magnetite concentrates, natural iron ore fines, magnesite, silicious bauxite, phosphate sands, coarse limestone and dolomite, and cement raw mix are some of the known materials that respond to this processing equipment. Each of these materials, because of intrinsic chemical and physical properties, reacts somewhat differently in this system. Balls formed from hematite or magnetite, for example, are fired at median temperatures of 2450 F, while dolomite and magnesite must be fired at temperatures above 3100 F. This difference does not merely mean that less fuel must be furnished the kiln for 2450 F, but such variation in firing temperature has a definite impact upon the operation of the grate and accessory equipment as well.

Data carefully recorded

The function of a pilot plant is to provide data that will enable the engineer to design full-scale machinery. To reduce capital investment for a required tonnage capacity, it is important that all components in the finished plant are precisely sized. The data required is derived partly by close observation, but principally by thorough pilot plant instrumentation.

In the traveling grate-rotary kiln system, these instruments consist of temperature and pressure indicators and recorders, and devices for measuring and recording solids and gas flows. Continuous analysis of gas composition, automatic proportioning equipment and the electrical means of accurately changing and controlling the operating speed of system components make the operation efficient.

A typical raw material for processing is specular hematite concentrates, produced by flotation and assaying 60-63 percent *Fe*. About 70 percent of the concentrates will pass

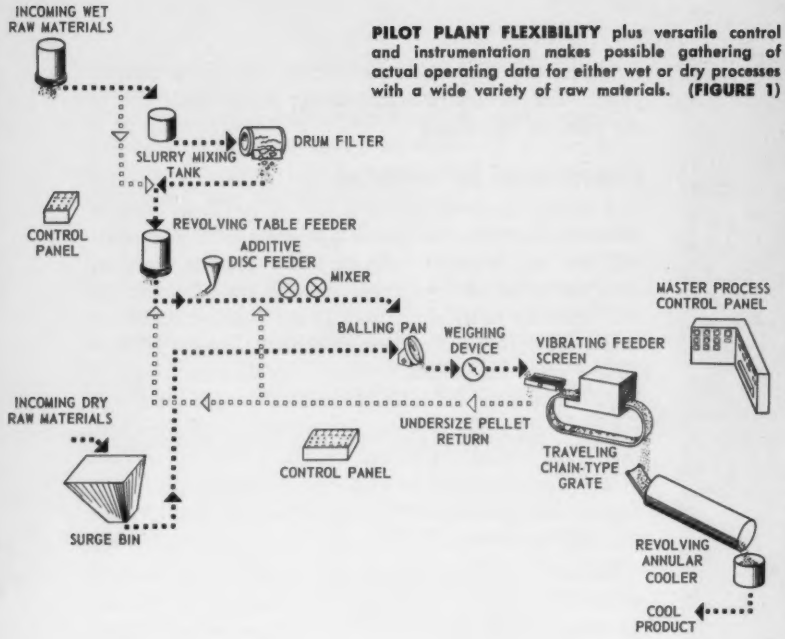

PILOT PLANT FLEXIBILITY plus versatile control and instrumentation makes possible gathering of actual operating data for either wet or dry processes with a wide variety of raw materials. **(FIGURE 1)**

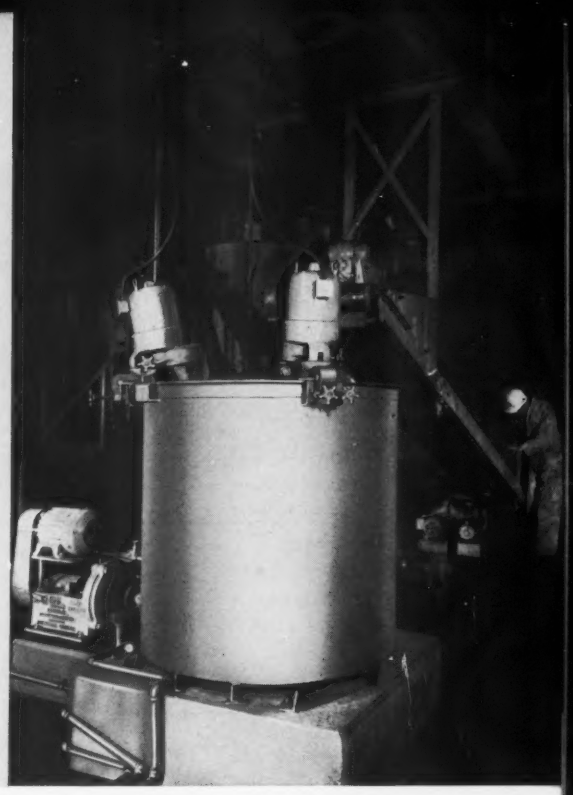

through a 325 mesh screen. The flow of material through the plant follows the diagram of Figure 1. Concentrates are brought to the wet materials handling room either in barrels or bulk. They are then dumped into a constant-speed table feeder which discharges to a conveyor, shown in Figure 2. The conveyor discharges into a slurry tank. Two high-speed, propeller-type mixers agitate the concentrate, and water is added in sufficient quantity to yield a pulp density of about 2 grams per milliliter.

The slurry is elevated by a solids pump and discharged into a drum filter tank. The rotating filter picks up the solids, dries them, and discharges a cake containing about 7 to 8 percent moisture. By carefully measuring pulp density and speed of the drum filter, cake moisture is held to an accuracy of plus or minus 0.5 percent, but not exceeding 8 percent.

The filter cake is conveyed to a specially designed table feeder mounted above an accurate, constant-speed weighing belt. A weigh cell senses the weight of feed passing over the belt and transmits a pneumatic signal to a receiver which controls the motor speed, thereby regulating the rate of table feeder discharge onto the belt. The rate of feed is remotely controlled by the balling pan operator by varying the reference pressure into the weigh cell.

The weighing belt discharges onto a conveyor belt which brings the specular hematite cake up to the balling pan. As the cake stream passes beneath the spout of a gravametric feeder, additives such as bentonite or limestone are deposited onto the cake. The rate of this gravametric feeder is manually adjusted to discharge a correct amount of additive according to the feed rate of the cake. An in-line mixing device, consisting of two rotating multi-bladed wheels, picks the cake and additive off the conveyor belt, violently disrupts it in a steel chamber, and lays it back onto the conveyor belt.

UNIFORM MOISTURE content for wet process is assured by addition of water in repulping tank. Raw material is brought from feed storage bin and table feeder, in the background, to the tank by conveyor belt. Slurry is then moved to the drum filter. **(FIGURE 2)**

Process is continuous

As shown in Figure 4, the granular cake then enters the balling pan at the one o'clock position. A portion of the cake forms seed pellets, while the rest of it mixes with the load and supplies the fine material required to build up ball size as seed pellets progress from the interior of the pan to the discharge lip. Water is added through spray nozzles to accomplish the balling action. The speed of the pan is readily changed through a variable-speed drive controlled manually by means of a crank. Varying the pressure in a hydraulic cylinder, whose piston is attached to a swivel on the back of the pan, readily increases or decreases the slope of the pan. With control of speed, slope and water at his instantaneous command, the balling pan

MATERIAL HANDLING AND PREPARATION are controlled from conveniently located control pulpit. The drum filter dewaters the slurry and discharges the solid material in the form of filter cake. The balling pan shown in the cover picture is in background. **(FIGURE 3)**

operator can continuously produce a ball of required diameter and physical characteristics.

Finished green balls fall from the pan to a conveyor belt and are conveyed to the weighing belt, shown in Figure 5, which registers the total weight of green balls fed to the traveling grate. Frequent sampling of green balls to determine moisture content facilitates later calculation of an accurate materials balance for a given test. The weighing belt discharges balls to a conveyor which is oscillated at the tail pulley. The balls are distributed uniformly across the conveyor belt and discharged onto a vibrating, rod-decked screen over its full width. The screen oversize, plus ¼ inch, is deposited on the traveling grate to a depth of 7 inches, while the undersize falls to a wide conveyor belt which discharges into a hopper. This hopper is tared on a weigh cell which transmits a pneumatic signal to a strip chart recorder on the master control panel. The weight of accumulating screen undersize is recorded on this chart.

BALLING, weighing, pellet sizing, grate feeding and incoming dry feed system are all controlled from this control console. Balling pan slope, speed and feed rate determine pellet size. (FIGURE 4)

Preheat carefully controlled

The interior construction of a typical traveling grate is shown in Figure 6. The chain-type grate pilot plant conveys the balls through a drying and a preheat chamber, each having its own windbox. A baffle extends from the roof structure to within an inch of the 7-inch-deep bed to divide the drying and preheat chambers. Gases at 1800 to 2000 F enter the preheat furnace from the rotary kiln. A high temperature fan (No. 1) draws the gases through the bed, into a hot cyclone dust collector, and then into the drying furnace. Ball temperature is reduced to about 700 F. The No. 2 fan draws the gases through the drying furnace bed and exhausts them out of the stack to the atmosphere at about 250 F.

Pressure taps are inserted into each furnace and its associated windbox. Thermocouples measure the gas temperature leaving each windbox and the gas temperature at the inlet of each fan. Measurements of static pressure in each furnace and windbox, differential pressure across furnaces and windboxes, and differential pressure across a furnace and its respective windbox, are indicated and recorded on the master panel. The fans are controlled from the master control panel by motor-operated inlet dampers. An eddy-current coupling, remotely controlled from the control panel, is used to govern grate speed. The flow of gas in the duct between the No. 1 fan and the inlet to the drying furnace is determined by measuring the differential pressure across an orifice plate. The waste gas flow is similarly determined. These differential pressures are indicated and recorded at the master control panel. To arrive at flow in terms of standard cfm, it is only necessary to read the delta *P* and the temperature of the gas, then read the flow off graphs.

Careful watch of pressures and temperatures is maintained during operation to assure that the hematite balls

GRATE-KILN SYSTEM of pilot plant provides accurate process data for designing full-scale commercial plants of the type shown. Units as long as 250 feet are now producing cement clinker. (FIGURE 5)

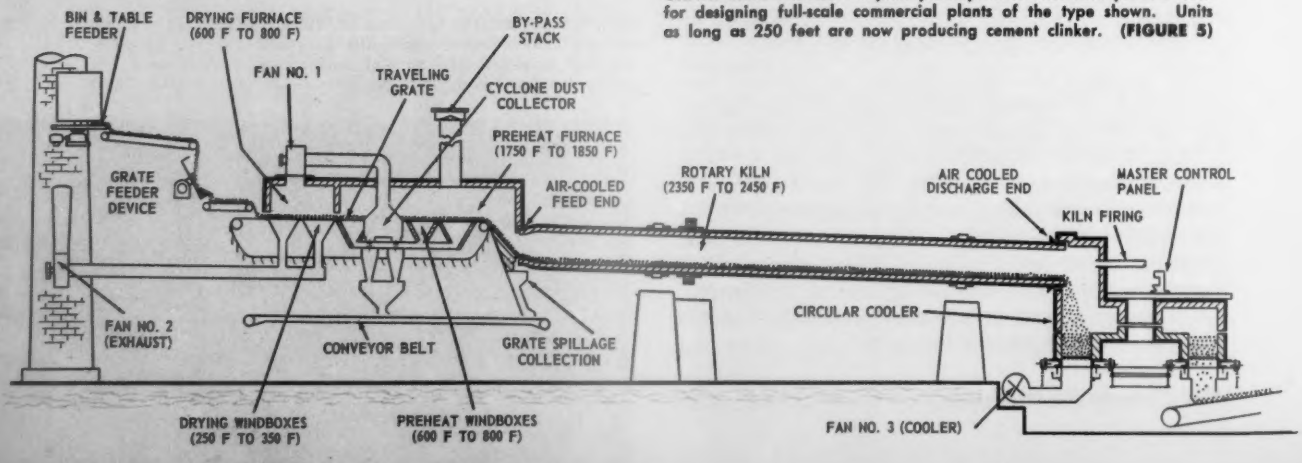
BIN & TABLE FEEDER
DRYING FURNACE (600 F TO 800 F)
FAN NO. 1
TRAVELING GRATE
BY-PASS STACK
CYCLONE DUST COLLECTOR
PREHEAT FURNACE (1750 F TO 1850 F)
GRATE FEEDER DEVICE
AIR-COOLED FEED END
ROTARY KILN (2350 F TO 2450 F)
AIR COOLED DISCHARGE END
MASTER CONTROL PANEL
KILN FIRING
CIRCULAR COOLER
FAN NO. 2 (EXHAUST)
CONVEYOR BELT
GRATE SPILLAGE COLLECTION
DRYING WINDBOXES (250 F TO 350 F)
PREHEAT WINDBOXES (600 F TO 800 F)
FAN NO. 3 (COOLER)

receive adequate heat-treatment on the grate, and also that the grate itself is not being overheated. The interior walls of the grate are refractory lined and the grate strand is protected by the heat absorption character of the feed material. The grate enclosure, with its front access and observation door, is shown in Figure 7.

The preheated balls are directed into the rotary kiln by cascading down a refractory-lined chute at the junction between the grate housing and the kiln. A water-cooled gas sample probe is inserted into this grate discharge area. A sample of the gases leaving the kiln is extracted constantly for continuous oxygen analysis. The oxygen content of the gas is recorded on the master control panel.

Temperature gradient determines heating

The balls proceed down the length of the small pilot kiln, shown in Figure 7, and are heated according to the temperature gradient that exists from the feed end to the discharge end. The kiln is pitched at a 3/8 inch slope. Retention time in the kiln is a function of feed rate and kiln speed, as the loading is held constant at about 7 percent. At the hot, or discharge, end of the kiln, the temperature of the kiln bed is measured by focusing a radiation pyrometer on the hottest area. This temperature is transmitted to an instrument on the master control panel and recorded on a circular chart.

The kiln discharge end is enclosed by the firing hood through which the kiln burner extends. The burner uses a mixture of air and propane gas. Air fed to the burner directly (primary air) and propane gas are metered through rotameters, shown on the master control panel at the extreme left.

The hot pellet discharge from the kiln falls into an annular, refractory lined cooler to a bed depth of about 20 to 30 inches. The cooler is rotated over multiple windboxes and air is introduced into a circumferential manifold and directed to vertical ducts that exhaust into the respective windboxes. The air supply to each windbox is controlled with plug valves.

Flow to each windbox is metered by measuring the pressure drop across an orifice plate. Pressure on each side of the orifice plate is transmitted through copper tubing to indicating and recording instruments on the master control panel. The delta *P* is read and the flow is determined from graphs. A portion of this cooling air is raised to high temperatures by extracting heat from the pellets and is introduced into the kiln to augment the primary air supply as well as to return useful heat to the process. The remainder is exhausted up the cooler stack after orifice metering. Product is discharged from the cooler through a vibrating feeder which feeds a conveyor belt. The conveyor belt takes the finished pellets to storage.

Data gathered from recording and indicating instrumentation throughout the entire pilot plant is expected not only to aid in mechanical designs of future full-scale plants, but also to provide the necessary information for determining plant power requirements. Motor types and sizes as well as control characteristics for specific processes can be selected on a more realistic basis.

BALLING PAN output is conveyed to weighing belt in background and then to vibrating feeder screen which uniformly distributes pellets across width of traveling grate. Pellets are preheated on grate before being discharged to rotary kiln below. **(FIGURE 6)**

ROTARY KILN completes the heat-treating of the pellets discharged from the grate. The process kiln product is discharged from the bottom of the firing hood into the annular cooler below. Cooler is instrumented to gather the needed data on heat recovery. **(FIGURE 7)**

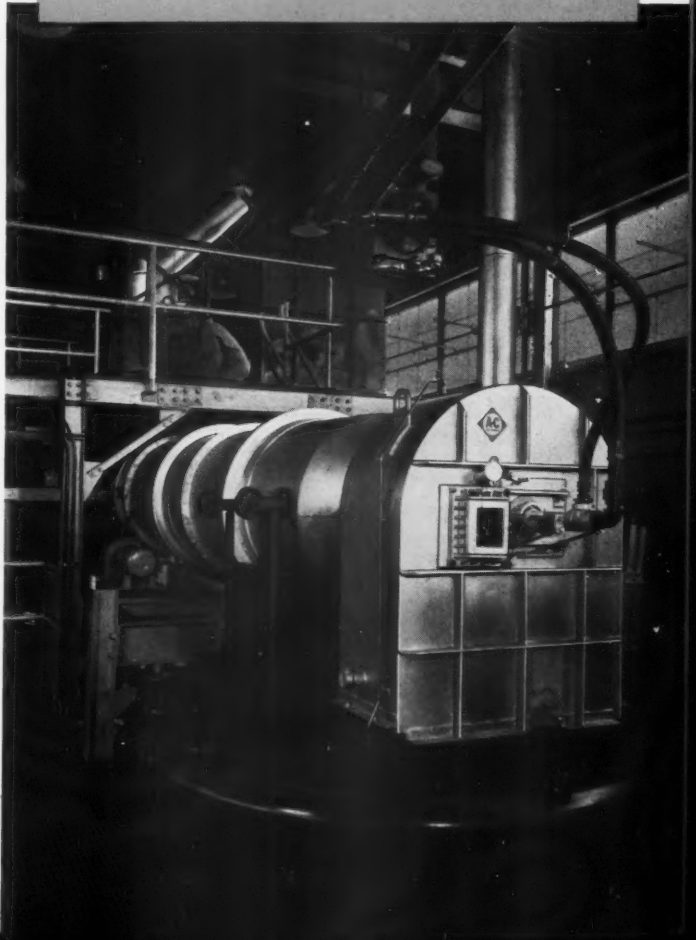

BALANCING THRUST IN SEPARATE TURBINE ELEMENTS

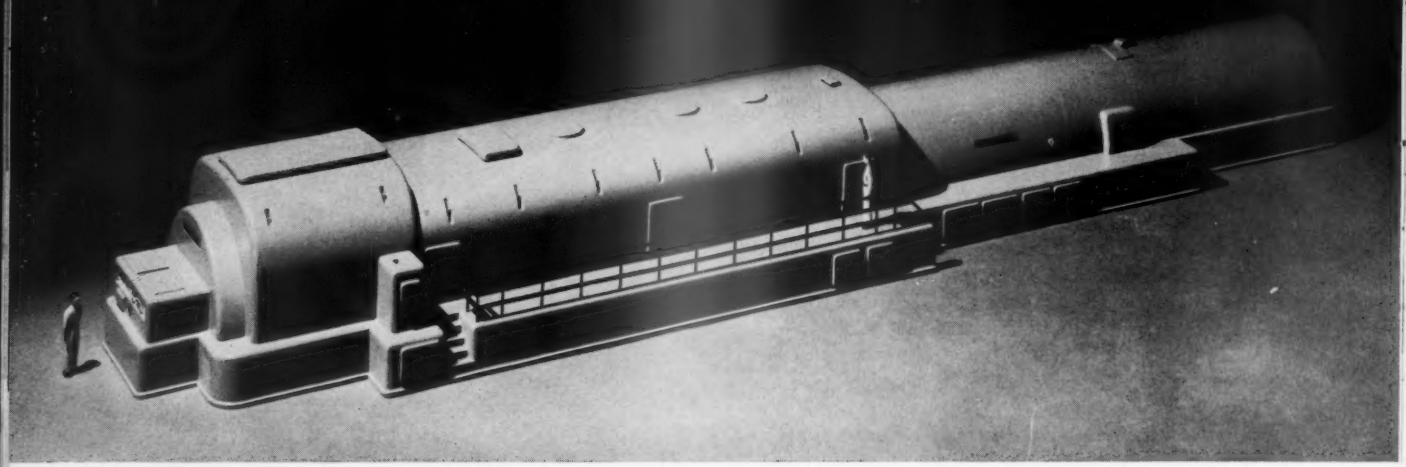

by **C. D. WILSON**
Chief Turbine Design Engineer
Steam Turbine Dept.
Allis-Chalmers Mfg. Co.

Opposed steam flow design reduces diameters of rotating elements in the high temperature region of large turbines.

THE PRINCIPLE of thrust balancing of individual turbine elements to obtain operating stability continues to be an important factor in turbine design, especially as turbine ratings become larger.

Balancing of individual turbine elements on the 220,000-kw triple-flow, tandem 3600-rpm reheat turbine in Figure 1 is accomplished by using opposed steam flow and by proportioning shaft diameters to balance major steam thrust by the pressures on the blades, as shown in Figure 2. The opposed-flow design favorably reduces diameters of the rotating elements in the high temperature region.

Moderately sized labyrinth-seal diameters in the diaphragms between opposed-flow sections and in the relatively low temperature shaft-end closures are designed to obtain the desired small axial thrust required to position the turbine shaft without float.

During operation, silica and other materials may separate from the steam and form coatings on the blading. When these deposits occur, they may alter the axial thrust by changing the steam pressure distribution inside a turbine. Since these conditions cannot always be avoided, and usually occur in specific areas, it is desirable to balance each turbine element separately, as shown in Figure 3.

To minimize change in thrust during all possible operating conditions, the turbine elements on each side of the reheat control valves must be designed to be nominally in balance. In the triple-flow turbine shown, these valves are located between the first and second turbines, each of which in itself is balanced.

Design evolves with unit size

The turbine shown in Figure 1 is rated at 220,000 kw with three parallel 26-inch exhaust flows and operates at 2000 psig, 1000/1000 F and 1½ inch Hg absolute exhaust pressure. It is covered by a sectional weather-tight housing for outdoor operation, with a weather-tight operating panel on the solidly bolted-down forward control pedestal.

Reheat intercept valves are enclosed in the weather-tight housing, while the front-located steam chest and the reheat stop valves are below the outdoor turbine deck. Side-crossunders connecting second and third turbines are permanently located beneath weather-tight side platforms and need not be removed during inspection and servicing.

The main thrust bearing is located on the solidly bolted-down No. 2 pedestal, and links connect the centerline-supported first and second turbine casings. Main steam inlet is to a separate ring-type nozzle chest, and the inner high pressure cylinder is centerline-supported, has built-in

OUTDOOR DESIGN of 220-mw triple-flow tandem turbine-generator unit for installation in Texas. Opposed steam flow in each of three turbine elements in this unit simplifies thrust balance. **(FIGURE 1)**

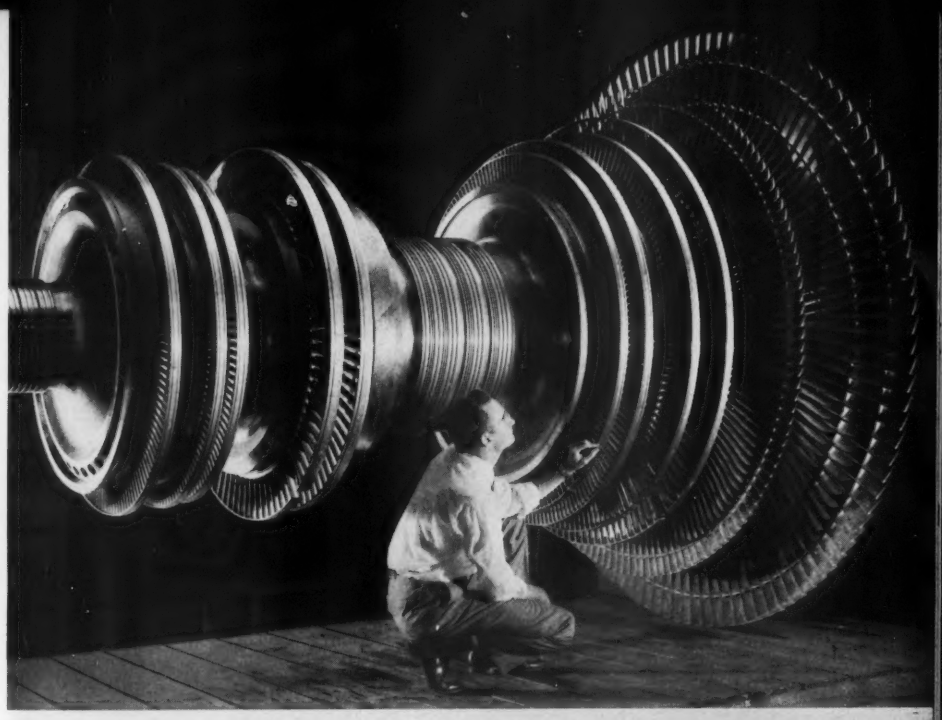

SECOND TURBINE SPINDLE includes (right) one low pressure blading section terminating in 26-inch blades and (left), in opposed flow, final intermediate pressure and initial low pressure blading. Center area seals to isothermal diaphragm which divides this turbine, separating areas of different temperature. **(FIGURE 2)**

FLOW OF STEAM in triple-flow turbine is given by arrows over the colored spindle cross sections. Flow is forward in the first turbine and to reheat, returning to opposed-flow intermediate pressure blading. High temperature is confined to this turbine. Intercept and back-up stop valves guard flow to the second turbine. In second turbine, forward flow is through remaining intermediate pressure blading, after which one third continues on through a few low pressure stages and through connecting pipes and the turbine opposed low pressure element. Two thirds of the low pressure flow in the second turbine passes through side-crossunders to the third turbine, which is double flow. All three low pressure flows exhaust through 26-inch blades to the condenser. **(FIGURE 3)**

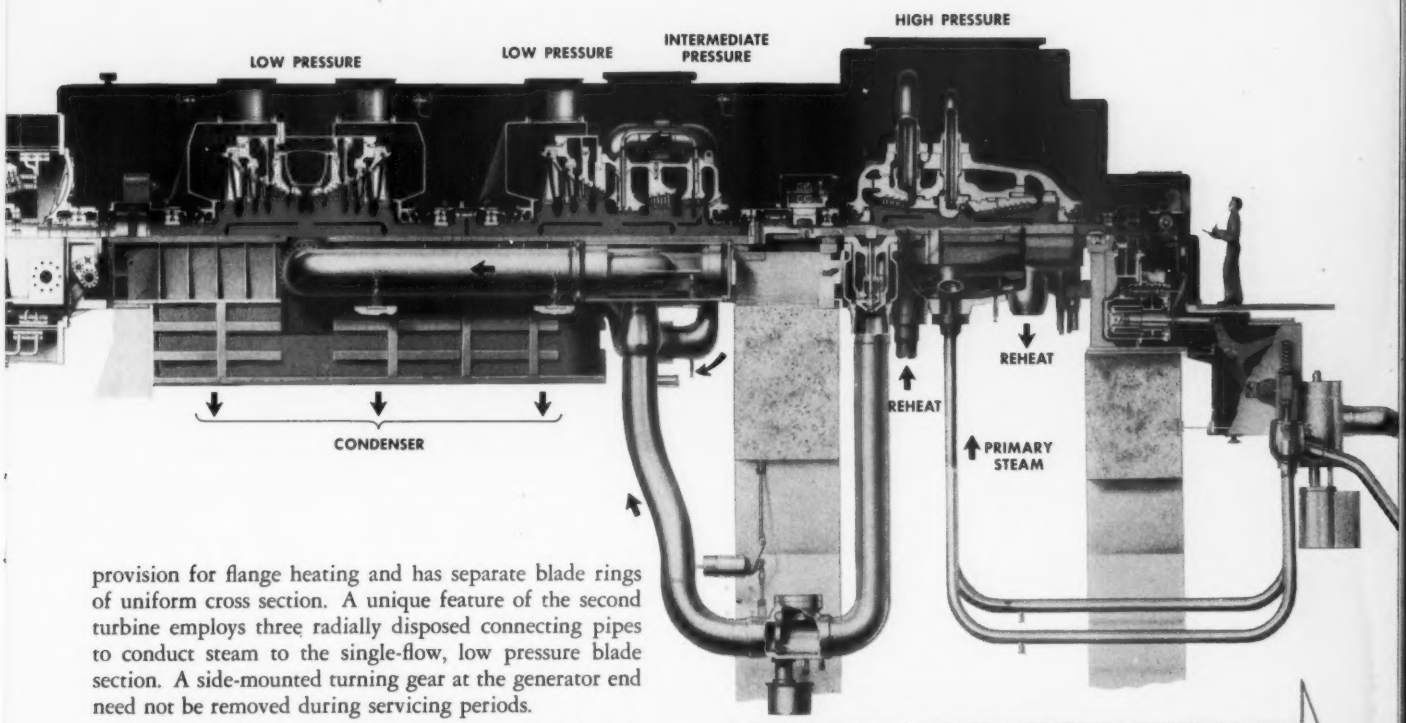

provision for flange heating and has separate blade rings of uniform cross section. A unique feature of the second turbine employs three radially disposed connecting pipes to conduct steam to the single-flow, low pressure blade section. A side-mounted turning gear at the generator end need not be removed during servicing periods.

Known principles, proven components plus the advances needed to obtain new higher ratings are making possible the variety of large turbine-generator units of today. The design parameters and station size limitations dictate the turbine arrangement required. Balanced thrust with opposed steam flow is one principle that will be applied in the newest large turbine designs.

OPPOSED-FLOW SPINDLES in triple-flow tandem 220-mw steam turbine is shown during one phase of assembly on the turbine test pit. High temperature is confined to the first turbine, foreground, and reheat control valves are installed in moderate temperature connection between first and second turbines. Side-crossunders are visible, joined to respective lower-half turbine casings. To minimize differential expansions, the thrust bearing for this machine is installed in the non-sliding pedestal between the first two turbines.

Allis-Chalmers Staff Photo by J. E. Gosseck

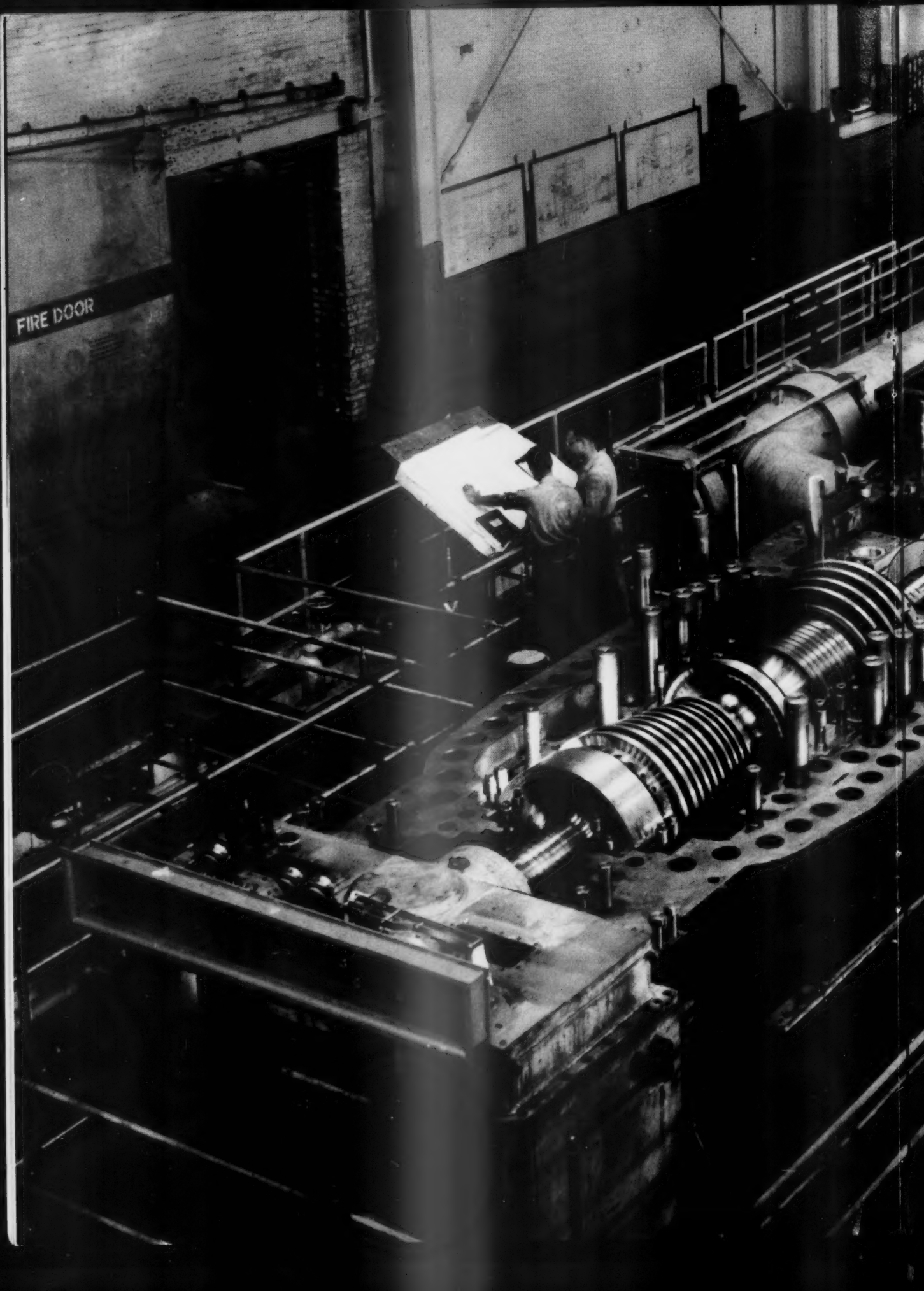
FIRE DOOR

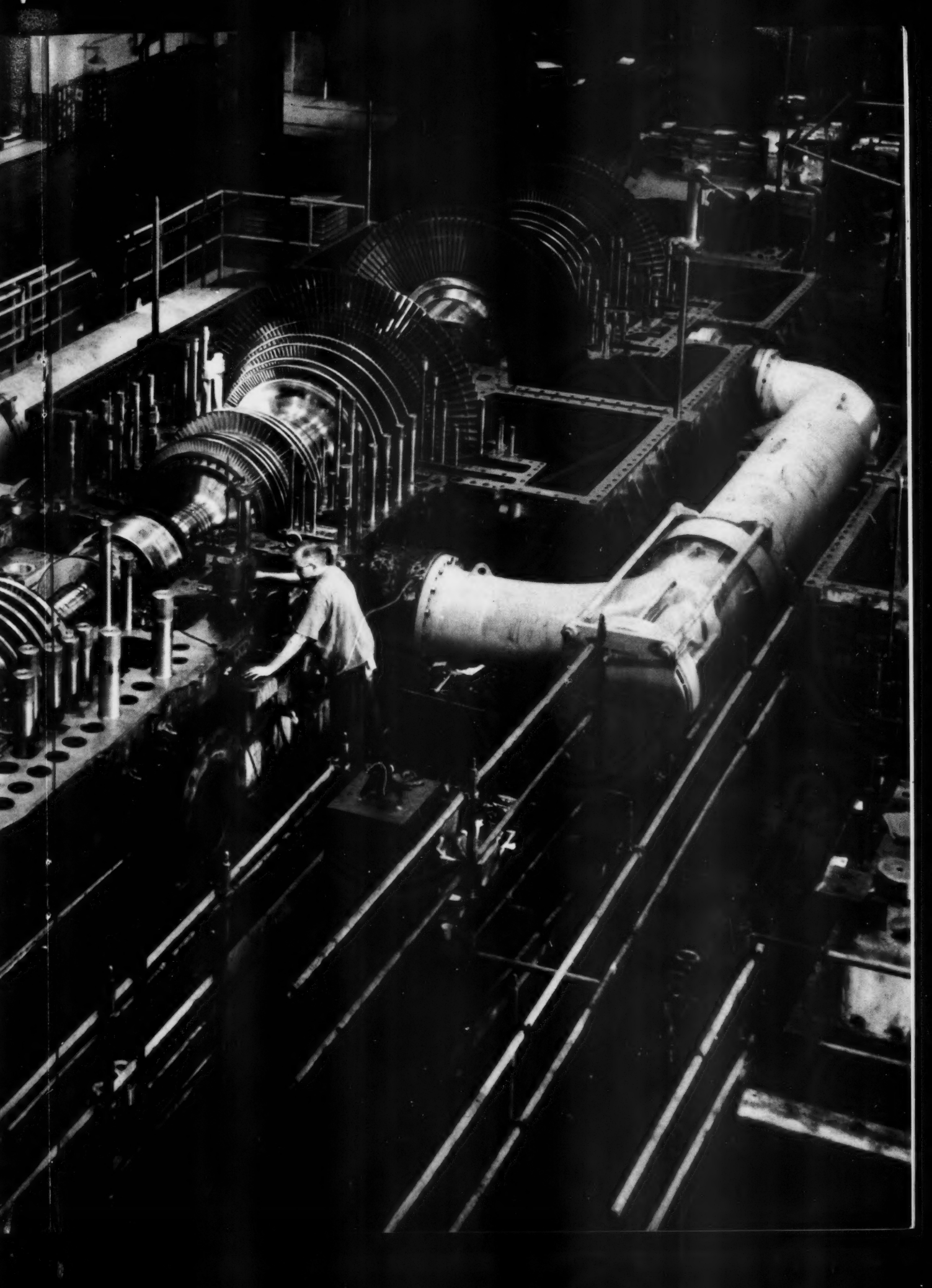

SINGLE PHASING THREE-PHASE MOTORS

by R. C. MOORE
Motor and Generator Dept.
Allis-Chalmers Mfg. Co.

Will a three-phase motor be damaged if it is accidentally operated on single phase? Here's what happens.

IF ONE LINE of a three-phase supply accidentally opens up, two questions immediately arise. Will vital machines keep running or must they be shut down? How much will the motor overheat if it is run on a single phase for a short period?

These questions can only be answered by reviewing three-phase motor characteristics and considering the changes that take place when one phase is opened. When a three-phase motor runs single phase, running torque, efficiency and power factor decrease; current, slip and heating increase; and starting torque is zero.

Several methods can be used to determine the effects of single phasing and many important performance characteristics of single-phase operation of a three-phase motor may be calculated. Symmetrical component analysis is most useful and utilizes familar techniques and constants.[1,2]

No-load, single-phase current is easily found

The no-load running current of an induction motor operating from a three-phase supply is readily expressed by the formula[3]

$$I_{3\ ph} = \frac{V_L}{\sqrt{3} \times Z_{po}} \qquad (1)$$

where V_L is terminal to terminal voltage and Z_{po} is the no-load motor impedance. A similar expression may be derived by means of symmetrical components to obtain the single-phase no-load running current:

$$I_{1\ ph} = \frac{V_L}{Z_{po} + Z_n} \qquad (2)$$

where Z_n is approximately equal to the three-phase locked rotor impedance:

When dividing equation (2) by equation (1)

$$I_{1\ ph} = \frac{\sqrt{3} \times Z_{po}}{Z_{po} + Z_n} \times I_{3\ ph} \qquad (3)$$

For high speed motors the no-load three-phase current can be as low as 16 percent of the full-load current. The per unit Z_{po} is then 6.67 per unit. With a locked rotor three-phase current of 650 percent, Z_n is 0.155 per unit.

For low speed machines the three-phase no-load and locked rotor currents may be 50 percent and 400 percent of full-load current. Z_{po} and Z_n are then 2.0 and 0.25, respectively, in per unit values.

Equation (3) can be rewritten as:

$$I_{1\ ph} = \sqrt{3}\left(1 - \frac{Z_n}{Z_n + Z_{po}}\right) I_{3\ ph} = AI_{3\ ph} \qquad (4)$$

where A varies from 1.70 to 1.60 approximately for high or low speed motors, respectively. However, appreciable

MACHINE RELIABILITY is most important in paper stock pumping operation where ambient conditions are severe. The white paper stock shown is often up to 95 percent water. If a three-phase motor should have to run single phase, the process would be interrupted.

variation of Z_n does not greatly affect the relation between single and three-phase no-load current. Therefore, a rough estimate can be made that the no-load single-phase current is slightly less than

$$I_{1\,ph} = \sqrt{3}\, I_{3\,ph} \qquad (5)$$

Calculations to determine the single-phase locked rotor current of a three-phase motor may be made using formula (1) except that Z_{po} is now replaced by Z_n. The full voltage single-phase locked rotor impedance of a three-phase motor may then be expressed by the following relation:

$$I_{1\,ph} = \sqrt{3}\frac{Z_n}{2\,Z_n} I_{3\,ph} = 0.866\; I_{3\,ph} \qquad (6)$$

where currents are locked rotor values.

The single-phase locked rotor current for a three-phase motor is, therefore, 86.6 percent of the three-phase locked rotor current.

Two-motor drive simulates single-phase operation

Many single-phase performance characteristics of a three-phase motor are not obtained by simple formulas as are no-load and locked rotor currents. However, for single-phase performance determination the actual three-phase motor operating from a single-phase supply, shown in Figure 1*a*, may be replaced by the two mechanically connected motors of Figure 1*b*. Each motor is identical to the actual motor of Figure 1*a* and operates from a three-phase supply. The stator windings of the two motors of Figure 1*b* are connected in series as shown and winding connections are made so that the air gap magnetic fields of the two motors rotate in opposite directions. With the motors thus connected, the torque output of the two-motor system is the difference of the individual motor torques.

From the two-motor arrangement, performance calculations such as torque, horsepower output, power factor, losses, may be made for single-phase operation. The advantage of the two-motor arrangement of Figure 1*b* is that familiar three-phase methods of calculation may be used for each motor and the results may then be combined to obtain the single-phase operating characteristics of the actual three-phase motor.

Circuit representation of the two series-connected motors may be made in the manner shown in Figure 2. At various speeds one motor labeled "positive sequence" develops more torque than the motor labeled "negative sequence" and determines which direction of rotation the two-motor system drives the connected load. At standstill, $s = 1.0$, because each motor develops identical torque in opposite directions and the net shaft output torque is zero. In Figure 2 the portion of the circuit from terminals A to C describes the positive sequence in a familiar three-phase circuit form.[4] The remaining portion of the circuit from terminals C to B similarly describes the negative sequence motor in the same familiar form. In the solution the complete circuit from terminals A to B may be reduced to a single impedance from which the current I_p and I_n may be determined from the impressed voltage V.

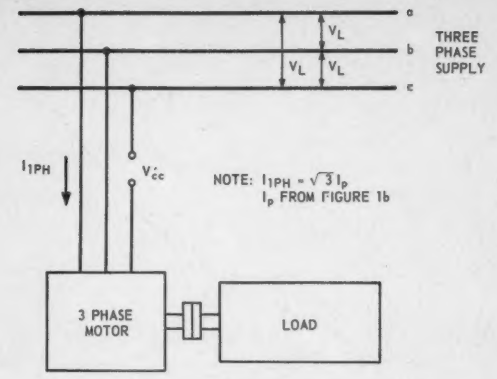

Figure 1a

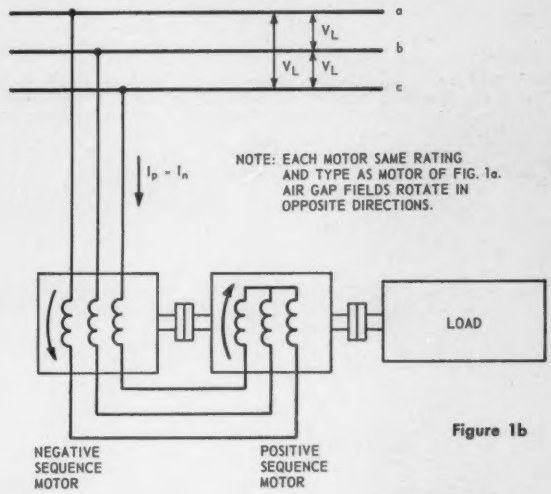

Figure 1b

THREE-PHASE motor operating single phase (1*a*) may be considered as two-series motor drive (1*b*) for performance evaluation. **(FIGURE 1)**

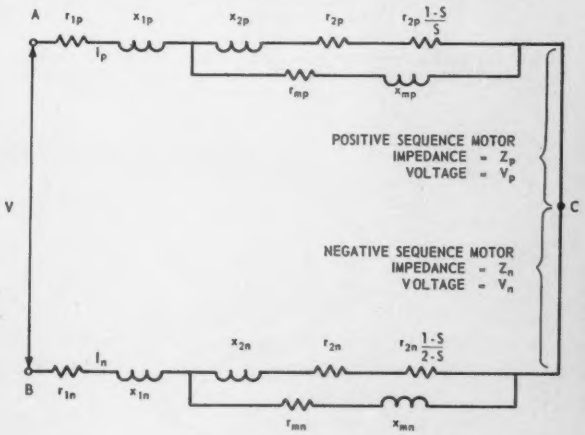

SYMBOLS

r,x = resistance, reactance, resp., ohms terminal to neutral
1,2 = primary, secondary, resp. (primary is usually the stator)
p,n = positive, negative, resp.
m = magnetizing
S = slip (slip rpm divided by synchronous rpm)
$V = V_p + V_n = V_L/\sqrt{3}$ NOTE: V_L from Figure 1.

CIRCUIT REPRESENTATION of the motors in Figure 1b helps to determine performance when operating single phase. **(FIGURE 2)**

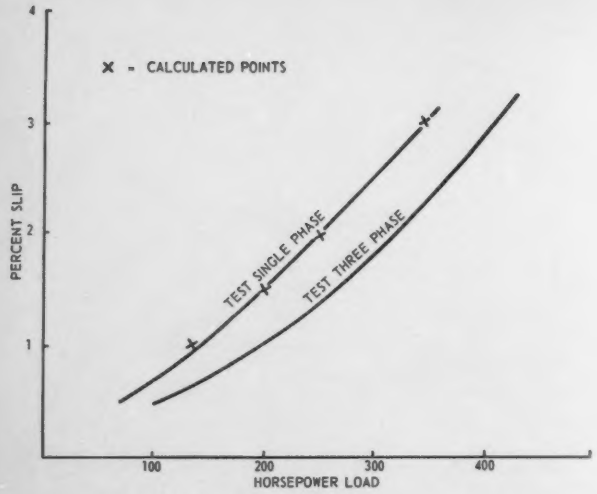

SLIP TEST curves indicate the speed change for both single and three-phase operation with various horsepower loads. **(FIGURE 3)**

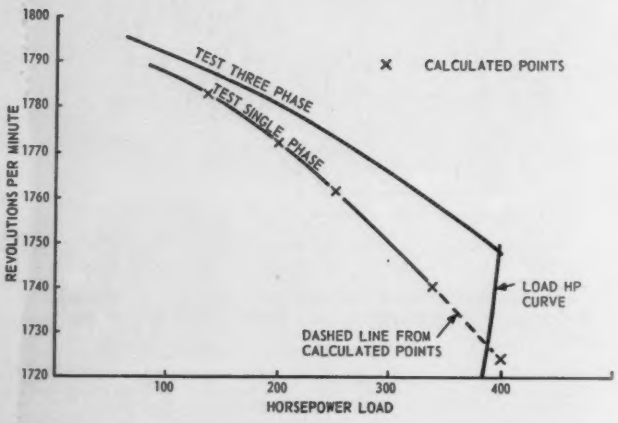

SPEED CHANGE curves show how speed changes for both single and three-phase operation for various horsepower loads. **(FIGURE 4)**

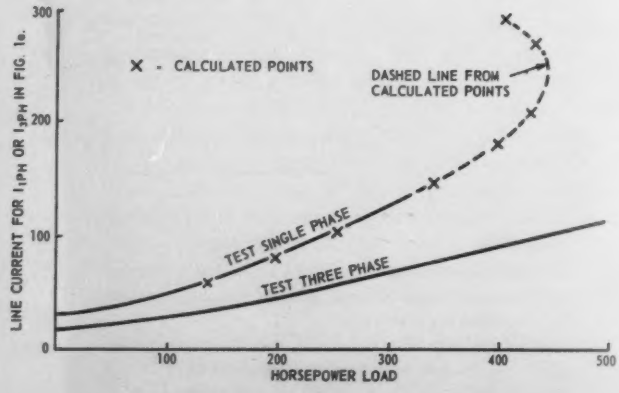
LINE CURRENT FOR I_{1PH} OR I_{3PH} IN FIG. 1a.
× - CALCULATED POINTS
DASHED LINE FROM CALCULATED POINTS
TEST SINGLE PHASE
TEST THREE PHASE
HORSEPOWER LOAD

CURRENT CURVES indicate the increase in line current encountered when operating a three-phase motor single phase. **(FIGURE 5)**

Single-phase operation is analyzed

Constants for a 400 hp, 1800 rpm, 220 volt three-phase squirrel-cage induction motor are studied to show how single-phase operating characteristics are found. For this motor (resistance and reactance values in ohms):

$r_{1p} = r_{1n} = 0.195$ stator resistance, terminal to neutral

$x_{1p} = x_{1n} = j1.47$ stator reactance, terminal to neutral

$r_{2p} = r_{2n} = 0.400$ rotor resistance, terminal to neutral

$x_{2p} = x_{2n} = j1.32$ rotor reactance, terminal to neutral

$r_{Mp} = r_{Mn} = 11.4$ magnetizing reactance, terminal to neutral

$x_{Mp} = x_{Mn} = j.71$ magnetizing reactance, terminal to neutral

$V = 2200/\sqrt{3} = 1270$ volts, terminal to neutral

s = slip = rpm difference between synchronous and operating speed divided by synchronous speed.

The rotor constants for the negative sequence motor are shown equal to those of the positive sequence motor. In some types of squirrel-cage induction motors using skin effect bars r_{2n} and x_{2n} may be different from r_{2p} and x_{2p}, since the rotor frequency of the negative sequence motor is much higher than the rotor frequency of the positive sequence motor.

If desired a further simplification may be made in the negative sequence portion of the circuit by removing the magnetizing branch. The parallel rotor branch impedance in this portion of the circuit is considerably smaller than the magnetizing impedance.

By assuming a value of slip, the complete circuit may be reduced to a single impedance consisting of a resistance and reactance in series. Current I_p, which equals I_n, may then be calculated from the impressed voltage V and the circuit impedance. The symmetrical components method shows that the desired single-phase line current, $I_{1\,ph}$, of the motor of Figure 1*a* is equal to

$$I_{1\,ph} = \sqrt{3}\, I_p \qquad (7)$$

where I_p is calculated from the equivalent circuit of Figure 2.

The individual motor horsepower and torque values may be determined for the portions of the circuit applying to each motor. Delivered shaft torque is represented by the difference of the motor calculated values, since the negative sequence motor torque subtracts from the positive sequence motor torque.

Single-phased motor current is larger

Using the circuit of Figure 2, calculated data for single-phase slip, speed and line currents are shown in Figures 3, 4 and 5. The data calculated apply to the motor in Figure 1*a* when operating single phase. The calculated points found from the circuit solution give results which predict very closely the test made on the 400 hp motor shown in Figure 1*a*. For comparison the normal three-phase test curves are also shown in the figures.

Figure 4 shows that for three-phase operation with a 400 hp load, motor speed is 1748 rpm. When one supply line is opened the motor operates single phase and will develop torque at 1728 rpm to carry 388 hp. Reference to Figure 5 shows that motor line current increases from 92 amps three phase to approximately double that amount for single-phase operation when one supply line is opened. Proper protective devices would then remove the motor from its supply to prevent excessive stator winding heating.

Voltage across series connected motors varies with speed

After calculating the impedances and the current of the two motors of Figure 1*b* represented by the circuit of Figure 2, the voltages across the two motors may be found.

When the motor speed changes from a lower to a higher value, the impedance of the positive sequence motor increases rapidly near the higher speed range accompanied by an increasing voltage across the motor as shown in Figure 6. Correspondingly the voltage across the negative sequence motor decreases as the speed increases. The fraction of the line voltage which appears across each motor may be expressed by the following relation:

$$V = V\left[\frac{Z_p}{Z_p + Z_n} + \frac{Z_n}{Z_p + Z_n}\right] \qquad (8)$$

The fraction $\frac{Z_p}{Z_p + Z_n}$ gives the per unit voltage across the positive sequence motor and similarly the fraction $\frac{Z_n}{Z_p + Z_n}$ gives the per unit voltage across the negative sequence motor. The impedances in the fractions are, of course, vector values. Calculated results from the circuit of Figure 2 are shown in Figure 6. The curves indicate that near full speed the braking torque developed by the negative sequence motor may be expected to be small since the voltage across the motor is small.

Power factor and efficiency are less for single-phase operation

Power and efficiency curves are plotted in Figures 7 and 8 for both single and three-phase operation of the 400 hp motor. The efficiency curves shown are from calculated data. For a given horsepower loading the efficiency for single-phase operation is less, as might be expected, largely because of the high stator line current and higher slip losses as compared to three-phase operation. Only two-thirds of the stator winding is in use during single-phase operation. However, the considerably larger line currents of single-phase compared to three-phase operation results in an overall stator copper loss being higher for the single-phase operation.

To find the shaft torque for single-phase operation of a three-phase motor, the two-motor system is again to be used with the equivalent circuit. Calculations to determine the torques of each motor may then be made and their difference taken to obtain the net output torque on a single-phase supply. The calculated speed-torque curves of Figure 9 show that in the normal operating range the braking torque of the negative sequence motor is very small compared to the torque developed by the positive sequence motor. The curves representing the torque contribution of each sequence motor and the resulting torques are shown. The net torque for single-phase operation is appreciably less than three-phase torque values. The two-motor system shows that a motor operating on single phase has no starting torque at standstill. Each motor develops the same torque but in opposite directions.

The torque curve in Figure 9 for the positive sequence motor may also be obtained by multiplying the three-phase values for a given speed in Figure 9 by the square of the percent voltage found from the upper curve of Figure 6.

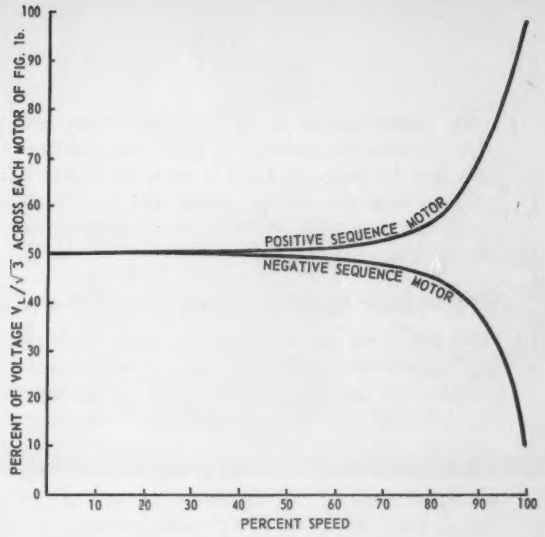

CURVES DEVELOPED from calculated data show the division of voltage across the two series motors in Figure 1*b*. **(FIGURE 6)**

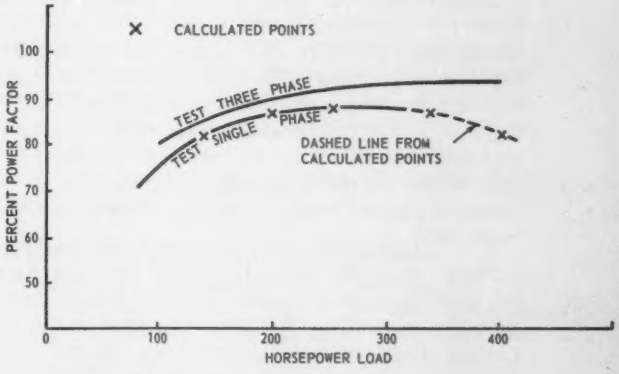

POWER-FACTOR curves show the changes in power factor that result when operating a three-phase motor on single phase. **(FIGURE 7)**

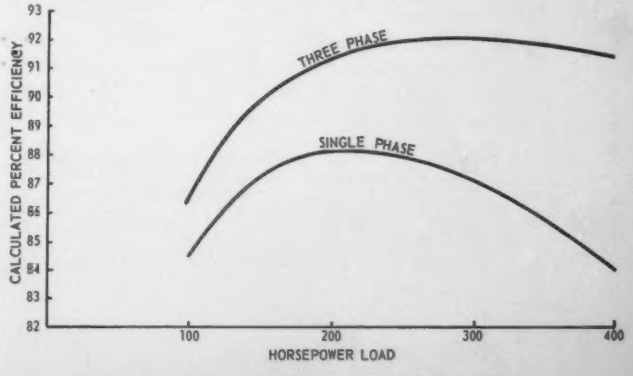

CALCULATED EFFICIENCY of normal operation and operation of the three-phase motor while single-phasing are compared. **(FIGURE 8)**

Breakdown torque of an induction motor for single-phase operation is considerably lower than for three phase. This may be expected from a study of Figure 6 which indicates that the voltage across the positive sequence motor and hence its torque decreases rapidly during the initial 20 percent speed drop.

Single-phase heating greater than three phase

Load losses are greater for single-phase than for three-phase operation. Stator and rotor copper losses may show considerable increase. In the 400 hp motor example being studied, the near full-load single-phase stator current is about twice the three-phase value. Since only two-thirds of the stator winding is used during single-phase operation, the ratio of the single to three-phase copper loss is $(2)^2 \times \frac{2}{3}$ or 270 percent considering only the current change. The loss may be further increased because resistance increases with temperature. The loss increase thus estimated does not, however, permit a direct evaluation of temperature rise of the stator winding on single phase, since the individual winding conductors on single operation are actually carrying twice the current, which is four times the conductor copper loss of three-phase operation.

Single-phase rotor losses are also greater than three phase for a specified motor loading. The negative sequence motor of Figure 1*b* develops rotor loss in producing a braking torque. This loss added to the positive sequence motor losses represents the total rotor loss of the motor of Figure 1*a* operating single phase. At a load of approximately 400 hp for the example being studied, the sum of the calculated single-phase rotor loss of both motors of Figure 1*b* was 250 percent of the normal three-phase value.

Motors with skin effect type rotor bars may have a resistance r_{2n} in the equivalent circuit of Figure 2 several times the value of r_{2p}. A range of r_{2n} three to five times r_{2p} may not be unusual. The rotor loss increase in such motors may be considerable. Therefore to properly evaluate the thermal capability of a three-phase motor on single-phase supply it is very important to know details of the motor design and construction.

Voltage between motor leads and disconnected power line may be high

Application of the method of symmetrical components may be made to find the voltage V'_{cc}, Figure 1*a*, across the open circuit between the motor terminal and the disconnected power line.[5] The open circuit voltage may be expressed as:

$$V'_{cc} = 3\ I_n\ Z_n = \sqrt{3}\ I_{1\,ph}\ Z_n \qquad (9)$$

The voltage V'_{cc} is shown in Figure 10 and is approximately proportional to the single-phase line current, since Z_n is essentially constant from standstill to full speed for the 400 hp motor tested.

The impedance, Z_n, of the negative sequence motor in Figure 2 with skin effect rotor bars may decrease from standstill to full speed. For this type of motor V'_{cc} may be slightly less at the higher speeds than shown in Figure 10.

The curve of V'_{cc} in Figure 10 may also be obtained by multiplying by 3 the lower curve of Figure 6 which represents I_nZ_n, the voltage across the negative sequence motor.

The normal three-phase characteristics of an induction motor may be considerably altered should one of the power supply lines be disconnected from the motor. In normal applications where the torque characteristics of the load increase with speed, the motor speed will drop slightly for single-phase operation. Accompanying the decrease in speed motor efficiency, power factor and breakdown torque decrease. Motor line current increase may be large, so that the motor will overheat because of the increased copper losses. When single phasing may be expected to occur, the motor should be protected by overcurrent devices, thermal relaying or other suitable means.

REFERENCES

1 *Symmetrical Components,* C. F. Wagner and R. D. Evans, McGraw-Hill Book Co., New York, N. Y., 1933.

2 *Application of the Methods of Symmetrical Components,* W. V. Lyon, McGraw-Hill Book Co., New York, N. Y., 1937.

3 "Proposed Standard for Induction Motor Letter Symbols," AIEE No. 58, January, 1956.

4 "American Standard Test Code for Polyphase Induction Motors and Generators," ASA C50.20-1954 (AIEE No. 500).

5 "Engineering Fundamentals," R. C. Moore, *Allis-Chalmers Electrical Review,* June, 1942.

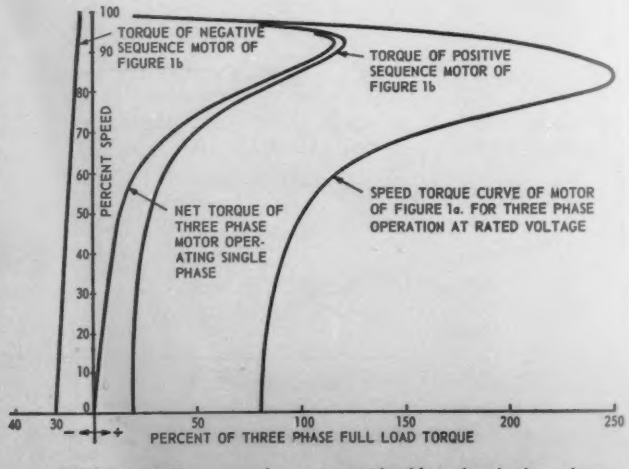
TORQUE OF NEGATIVE SEQUENCE MOTOR OF FIGURE 1b
TORQUE OF POSITIVE SEQUENCE MOTOR OF FIGURE 1b
SPEED TORQUE CURVE OF MOTOR OF FIGURE 1a. FOR THREE PHASE OPERATION AT RATED VOLTAGE
NET TORQUE OF THREE PHASE MOTOR OPERATING SINGLE PHASE
PERCENT SPEED
PERCENT OF THREE PHASE FULL LOAD TORQUE

SINGLE-PHASE torque values are considerably reduced when phase is opened and three-phase motor operates single phase. **(FIGURE 9)**

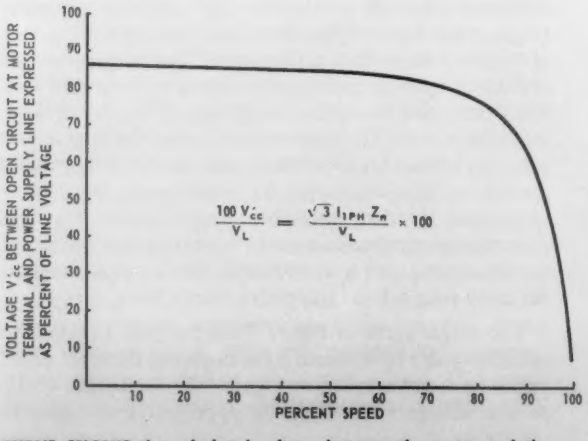
VOLTAGE V_{cc} BETWEEN OPEN CIRCUIT AT MOTOR TERMINAL AND POWER SUPPLY LINE EXPRESSED AS PERCENT OF LINE VOLTAGE
$\frac{100\ V'_{cc}}{V_L} = \frac{\sqrt{3}\ I_{1PH}\ Z_n}{V_L} \times 100$
PERCENT SPEED

CURVE SHOWS the calculated voltage between the motor and the broken supply line when single-phase operation occurs. **(FIGURE 10)**

Determining Thermal Transients

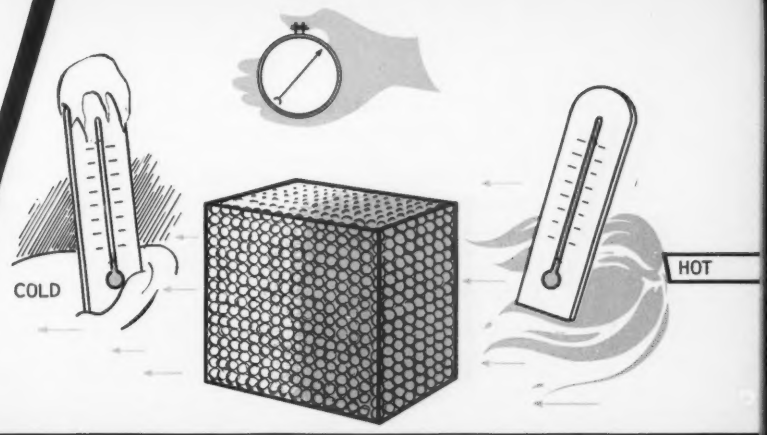

MOVEMENT OF HEAT through even a simply shaped body becomes important when its transient time becomes critical. Modern design practice requires an accurate determination of transient heat.

by W. O. VEBBER
Engineering Analysis Section
and
T. R. HERMAN
Nuclear Pump Section
Allis-Chalmers Mfg. Co.

By comparing heat flow to electric current, thermal distribution problems can be solved electrically. Sample calculation illustrates method.

TODAY'S EMPHASIS on the higher operating efficiency and extended application of machines frequently means that their elements must be redesigned for high temperature environments. To meet these more stringent conditions, the temperature distribution within a device must be known.

Prior to the introduction of high speed computing equipment, thermal analysis was seldom undertaken except on the basis of previous experience or test results. With analytical calculations made possible by the digital computer, the thermal characteristics of equipment can be predicted without building expensive working models and superior performance is the result.

Many problems encountered in present engineering practice are impossible to solve by classical methods. It is only by using a computer and numerical methods that general solutions describing the interaction of physical laws can be made available to the engineer. There is no limit to the scope of the thermal problems that can be solved by a digital program. Problems involving nuclear reactors, rotating electrical equipment and critical fluid pumps are typical.

Complete description defines the problem

Thermal analysis is a consideration of the heat flow relative to an object — either heat in the body itself or resulting from outside influences. Many applications now demand precise and accurate measurement of the temperature in an assembly during normal and emergency operation. The scope of an actual problem makes it impractical for ordinary mathematics to produce more than an approximate indication of the true situation without the aid of a high speed digital computer. Suppose that the edges or boundaries of a particular machine component or structural element have a specified temperature at a given time. Considering heat generation and removal, what is the temperature at any interior point at any later time?

The component may be a composite one, consisting of materials which transmit heat with varying conductivities. Moreover, heat may be stored within the component. Certain devices, such as electrical equipment or nuclear

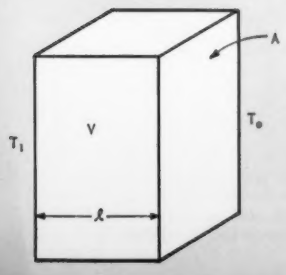

SKETCH shows thermal condition where material length is ℓ, cross-sectional area is A and volume is V. Three-dimensional analysis follows a similar arrangement. **(FIG. 1)**

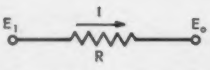

VOLTAGES E_i and E_o are applied to resistor R to produce the current I. **(FIG. 2)**

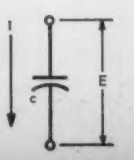

CURRENT I through an electrical capacitor is related to C, the value of the capacitor and the time rate of change (dE/dt) of the voltage drop, E, across the capacitor. **(FIGURE 3)**

reactors, produce additional heat internally because of their operation, which alters their internal temperature distribution.

Before a numerical computer can be brought to bear on this problem, some method must be found:

a — To describe to the computer the geometrical shape of the body under study.

b — To describe the nature and relation of the materials forming the body. This must include how readily they store and transmit heat.

c — If sources of heat are present, their location and degree of intensity must be described.

d — The initial value of the temperatures within and on the body must be outlined.

e — A mathematical model of the physical process of heat transmission must be set up.

f — Major considerations are the conduction and convection conditions, and the film coefficients between the fluid and the surface to be cooled must be known.

Electrical analogy analyzes heat flow

Because of the numerical restrictions of digital computer operation, methods which can be programmed must be invented to accomplish steps *a* through *f*.

All currently useful methods are based on the finite difference approximations. Thus complicated problems can be broken up into sequences of simple calculations which a digital computer can be instructed to perform.

Once the thermal analysis has been stated in finite difference terms, sets of simultaneous algebraic equations may be set up involving the temperatures at discrete points inside the body. These equations may be solved all at once or by a series of successive approximations.

It can be shown that there is a formal analogy between the equations of heat transfer in finite difference terms and those describing a simple electrical network. For example, consider a slab of some heat-conducting material with temperature T_1 on one side, T_0 on the other, as shown in Figure 1.

The law of heat conduction that applies is:

$$q = (T_1 - T_0)\, K \frac{A}{l} \qquad \text{Eq. (1)}$$

where q = the quantity of heat flowing through the body.

K = a physical constant of the material, called its "thermal conductivity."

Observe that for a given K and fixed temperature difference $(T_1 - T_0)$, q will decrease if l is increased, and likewise q will increase if A (surface area) is increased.

With Eq. (1) written as:

$$q = \frac{T_1 - T_0}{\frac{l}{KA}} \qquad \text{Eq. (2)}$$

let l/KA, a constant for a fixed shape and size of given material, equal R_T,

then $$q = \frac{T_1 - T_0}{R_T} \qquad \text{Eq. (3)}$$

where $R_T = l/KA$, the thermal resistance of the slab in Figure 1.

Heat transfer by mass transfer also has an electrical equivalent. The heat transfer is given by

$$q = V\rho A c_p (T_1 - T_0)$$

where V = the velocity of fluid flow.

A = the cross-sectional area of the flow path.

ρ = density of pumped fluid.

c_p = specific heat of fluid.

The thermal resistance in this case is

$$R_T = \frac{1}{V\rho A c_p}$$

When convective films are involved, they can be handled in a similar manner. The resistance R_T is equal to the reciprocal of the product of the film coefficient and the area.

$$R_T = \frac{1}{h_c A}$$

As the thermal resistance increases, the thermal "current" q will decrease (if $T_1 - T_0$ is fixed) and vice versa. This is analogous to the behavior of the electrical current in the single circuit of Figure 2.

Since Ohm's Law is $$I = \frac{E_1 - E_0}{R} \qquad \text{Eq. (4)}$$

the following association results:

T_1, Fixed outer temperature.....E_1
T_b, Unknown inner temperature.....E_b
T_0, Fixed outer temperature.....E_0
$\rho c_p V$, Equivalent heat capacity of body.C
$\frac{1}{2}$ (l/KA), Equivalent resistance of body.$R_1 = R_2$*

*R is split in two halves, half "going in" and half "going out."

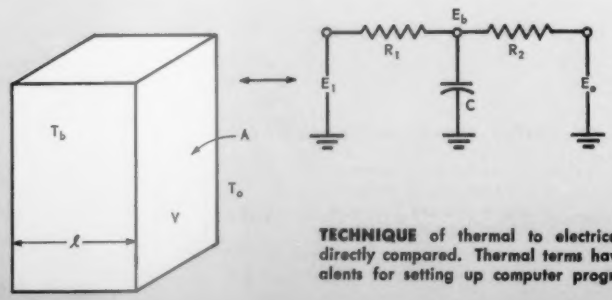

TECHNIQUE of thermal to electrical development is directly compared. Thermal terms have electrical equivalents for setting up computer program. **(FIGURE 4)**

TABLE I

Thermal	*Electrical*
Temperature T	Voltage E
Heat Flow q	Current Flow I
Thermal Resis. l/KA	Electrical Resistance R
Heat Conduction (Fourier's Law)	Ohm's Law

The analogies in Table I contain the necessary basic ideas to analyze, in discrete terms, any heat-transfer problem with constant temperatures (with respect to time). However, transient (or time-varying) problems need further consideration. The basic equation of heat storage in material bodies is

$$\triangle Q = mc_p \triangle T \qquad \text{Eq. (5)}$$

where

$\triangle Q$ = the quantity of heat stored in the body.

m = the mass of the body.

c_p = a physical constant of the material called the "specific heat capacity."

$\triangle T$ = the change in temperature of the body above a reference.

Let the density of its material, in Figure 1, be ρ. Since

$$m = \rho V$$

then Eq. (5) becomes

$$Q = \rho V c_p \triangle T \qquad \text{Eq. (6)}$$

In some time interval $\triangle t$, the time rate of change of $\triangle Q$ is

$$\frac{\triangle Q}{\triangle t} = \rho V c_p \frac{\triangle T}{\triangle t} \qquad \text{Eq. (7)}$$

therefore $\frac{\triangle Q}{\triangle t}$ is heat quantity per unit of time. q is also heat quantity per unit of time, therefore

$$q = \frac{\triangle Q}{\triangle t} \text{ or } \rho V c_p \frac{\triangle T}{\triangle t} \qquad \text{Eq. (8)}$$

Since $\rho V c_p$ is another constant relative to a piece of material, it can be given a new symbol C_T;

therefore

$$q = C_T \frac{\triangle T}{\triangle t} \qquad \text{Eq. (9)}$$

For infinitesimally small increments, Eq. (9) becomes

$$q = C_T \frac{dT}{dt} \qquad \text{Eq. (10)}$$

Equation (10) is the differential equation of heat storage of our element. An electrical analogy of Eq. (10) exists according to Figure 3.

Table II is an association of transient thermal and electrical considerations.

TABLE II

Thermal	*Electrical*
Thermal Capacity $\rho V c_p$	Electrical Capacity C
Rate of Change of Temperature $\frac{dT}{dt}$	Rate of Change of Voltage $\frac{dE}{dt}$

The two basic equations of a thermal transient problem are now in two forms, thermal and the analogous electrical form.

Heat storage has electrical equivalent

In most practical problems, only one temperature is associated with a slab, arbitrarily assumed as some sort of average temperature, for example, at its center. Then any slab of material may be approximated as shown in Figure 4.

Complex thermal analysis problems break down into electrical networks of interconnected resistance-capacitance elements in which the electrical components incorporate the material and geometrical properties, while the voltages and currents model the temperatures and heat flows.

Using an electrical network analogy is advantageous because much work has already been done on the digital computer solutions of electrical network problems involving resistance networks. However, the introduction of the capacitor (heat storage) is an aspect not usually present in electrical network studies and must be included. Normally Kirchoff's current law is applied at each point where two or more branches join. Kirchoff's Law of Currents states that the algebraic sum of all currents at any circuit junction must be identically zero.

$$\sum_{n=1}^{k} I_n = I_1 + I_2 + I_3 + \cdots\cdots + I_k = 0$$

In thermal terms:

$$\sum_{n=1}^{k} q_n = q_1 + q_2 + q_3 + \cdots\cdots + q_k = 0$$

The current I_k in any branch including a resistor is of the form of Eq. (4).

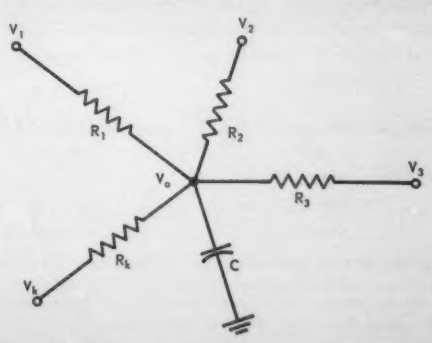

CAPACITOR changes formation of the sum of network current. **(FIG. 5)**

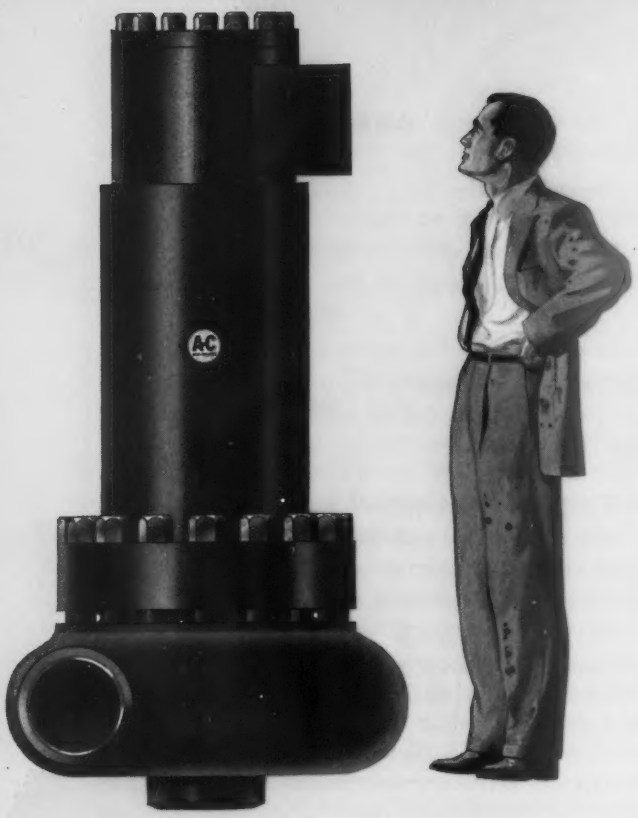

CANNED MOTOR-PUMP for the recently launched *N. S. Savannah* will handle radioactive water in the reactor cycle. **(FIGURE 6)**

If the storage or capacitive addition of Figure 5 is considered, the result is

$$Ic = C_0 \frac{dE_0}{dt} \qquad \text{Eq. (11)}$$

Therefore Kirchoff's current law must be modified slightly to account for the possibility of storage at the element in question, that is,

$$\sum_{n=1}^{k} I_n - I_c = 0 = I_1 + I_2 + \cdots + I_k - I_c$$

or, using Eqs. (4) and (11),

$$\frac{E_1 - E_0}{R_1} + \frac{E_2 - E_0}{R_2} + \cdots + \frac{E_k - E_0}{R_k} = C_0 \frac{dE_0}{dt}$$

or Eq. (12)

$$E_1/R_1 + E_2/R_2 + \cdots + E_k/R_k = C_0 \frac{dE_0}{dt} + \left(\frac{1}{R_1} + \frac{1}{R_2} + \cdots + \frac{1}{R_k}\right) E_0 \qquad \text{Eq. (13)}$$

An equation similar to Eq. (13) must be written for each junction point in the equivalent electrical circuit, and the digital computer must be programmed to solve this large set of equations.

The derivative term $C_0 \frac{dE_0}{dt}$ may be replaced by an approximate form, that is,

$$C_0 \frac{dE_0}{dt} \qquad C_0 \left(\frac{(E_0^{k+1} - E_0^{k})}{\triangle t}\right) \qquad \text{Eq. (14)}$$

where E_0^{k} = the "old" value of E_0 and E_2^{k+1} will be the "new" value on the next iteration.

The substitution of Eq. (14) into Eq. (13) results in

$$E_1/R_1 + E_2/R_2 + \cdots + E_k/R_k = C_0 \left(\frac{E_0^{k+1} - E_0^{k}}{\triangle t}\right) + \left(\frac{1}{R_1} + \frac{1}{R_2} + \cdots + \frac{1}{R_k}\right) E_0^{k+1} \qquad \text{Eq. (15)}$$

The computer can then be told to set up Eq. (15) at every junction of the network. It can then solve for E_0^{k+1}, the latest value of voltage analogous to temperature at the desired point, and move from point to point in the thermal equivalent circuit. In this manner increasingly accurate series of successive approximations to the transient thermal problem result.

An important addition to the above analysis must be considered if there is heat generation present in the material under study. Examples of this are nuclear reactor fuel elements, where fissionable materials not only conduct heat but generate it as well, and in electrical current-carrying coils, where heat is generated by resistance to the current flow. In such cases it is only necessary to add a current at each junction point, equal to the heat source present in the element.

Critical operation proves method

Other additions involve programming the computer to cause certain of the temperature analogous voltages to follow a predetermined set of values. This is necessary when the study of cyclic thermal transients is undertaken.

The importance of accurate heat-transfer analysis is demonstrated in a consideration of the development of a canned motor-pump serving a nuclear reactor. The pump unit circulates the hot, high pressure primary water through the reactor vessel and primary heat exchanger. Because the water is radioactive, the unit must be completely leak-tight. Despite the stringent operating requirements, the unit must be absolutely dependable. A canned motor-pump is shown in Figure 6.

The motor rotor operates in a cavity which is completely filled with the high pressure primary water. As a consequence, the motor stator is totally sealed in a pressure shell, which prevents the use of air cooling as in conventional motors. The stator is cooled by an integral heat exchanger that maintains desirable operating temperatures. Figure 7 is a sectional view of the assembly.

The first part of the thermal problem required a determination of temperatures at all points within the stator when the pump is operating at steady state, with the cooling system operating normally.

The stator was divided into finite sections for analysis, and because the unit is symmetrical, only one half-slot was studied, with heat flow in longitudinal and radial directions. The thermal conductivities and boundary layer heat-transfer coefficients were calculated by using established values and conventional methods. Heat removed by the water circulation was simulated by considering the thermal properties of the water and the flow rate.

The generated heat came from several sources, which were calculated and added to the system in the locations where they actually occurred. During normal operation the heat capacities of the unit are not important because the heat transfer is constant.

The normal steady-state temperatures were formerly calculated by laborious, longhand methods, which of necessity included simplifying assumptions. These relationships are presently solved by setting up the equivalent electrical circuit with the easily calculated conductances and heat-source values. An equation is written about every point or segment. The solution gives the temperature at every point within the stator when the heat generated equals the heat removed. Figure 8 shows a circuit used in a typical problem.

Emergency conditions are predicted

What would happen if the external coolant supply to the pump unit were interrupted? The heat generation would be unchanged, but it would all contribute toward heating up the unit. To find the unit's heat capacity the same network is used that solved the static condition, but the heat capacity of every junction was calculated to include an additional equivalent capacitance at every point. With the initial steady-state conditions as the starting point and the heat capacity represented, all the temperature-time relationships are calculated.

The resulting mass of equations was solved by the computer. Successive temperature approximations were printed out each minute, and the problem was solved continually until a printout showed that the stator temperature had reached the allowable limit. Then the computer registered the total time the pump unit could be operated without external coolant.

To demonstrate the flexibility of computer solutions, by removing the capacitances simulating the water trapped in the motor coolant jacket, the safe operating time without the added heat sink could be calculated.

The digital computer completely answered the questions relating to the temperature conditions in the canned motor-pump during normal operation and during coolant shutdown. Thus the operating procedure for the reactor plant can take an important safety factor into account. With an external coolant failure, the pump unit will operate safely for several minutes while flow is being restored.

What used to be considered normal temperature in many areas is not now applicable. Precise evaluation of heat transients is often required when new equipment is made smaller and with increased ratings. Industrial machinery is being called upon to drive heavier loads, with intense emphasis on smaller equipment. Nuclear plant operation requires an exact knowledge of the thermal capabilities of the core enclosure, and of all control and auxiliary equipment. New metallurgy and fuel research initiated the space age, but the electronic computer produces the information that insures its progress. Precise thermal analysis has proved to be all important in maintaining the advance of modern technology.

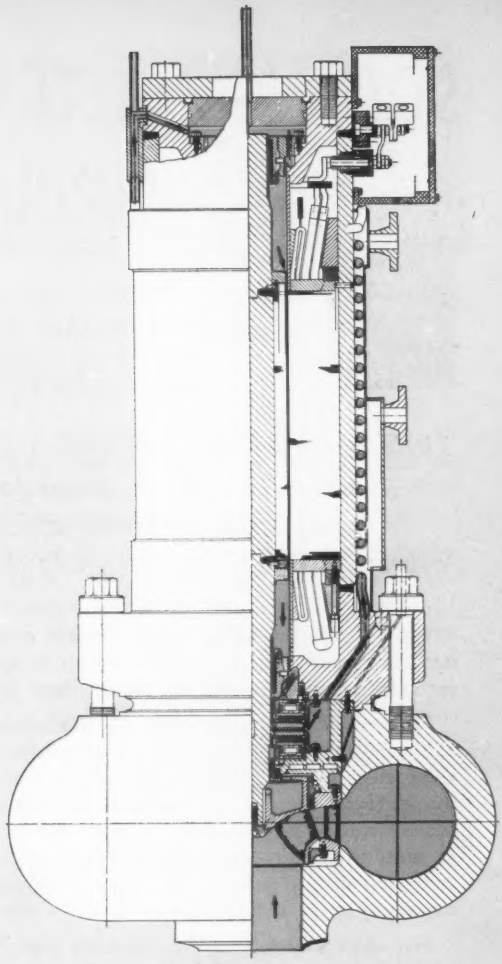

ENTIRE MOTOR operates completely submerged in the primary water. Liners, or "cans," in the bore between the rotor and stator protect these elements from the fluid. The stator is cooled to operate below the 200 C hot-spot temperature of Class H insulation. Since the motor is enclosed in the pressure-containing outer shell, it is as small as possible to meet horsepower requirements. The result is a higher than normal heat loss per unit volume. An auxiliary impeller circulates the water through the water-lubricated bearings, the gap between the rotor and stator and a cooling coil wrapped around the stator liner. External motor coolant passes over the cooling coil and removes heat generated by the motor. **(FIGURE 7)**

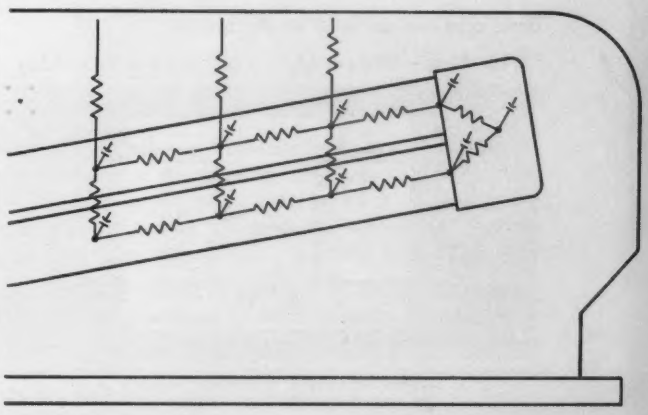

SIMPLIFIED LAYOUT of an equivalent circuit represents actual machine section with resistors as thermal conductors and capacitors as heat absorbers. The resulting voltages at junction points are equivalent to actual temperatures occurring in the machine. **(FIGURE 8)**

SOLVING MULTI-WINDING TRANSFORMER CIRCUIT PROBLEMS

by A. H. KNABLE
Switchgear Dept.
Allis-Chalmers Mfg. Co.

Little known method of circuit analysis makes possible solutions to transformer problems which otherwise would be extremely difficult.

WHEN CONSIDERING all the possible winding connections that are used today, the need for an approach to problems involved in applying transformers is apparent.

Problems of voltage regulation, breaker rating, relaying and sizing transformer windings represent some of the areas which require a knowledge of multi-winding transformer circuit theory. The method of solving such problems involves a general equation which can be expressed in terms of a summation sign and general subscripts. Interpreting details such as signs and terms represents a stumbling block in the application of the equation.

Five examples are given to provide a working knowledge of the equations. Understanding these practical applications of the equations will aid in solving many similar problems.

Example 1 illustrates the flexibility of both per unit (P_u) and ohmic representation of terms, and also brings out the interpretation of signs in the equation. Example 2 illustrates the simplicity of applying the equation to autotransformer connections. Example 3 is a practical problem solved by the general equations. Example 4 illustrates the use of the equations in calculating equivalent impedances for solving circuit problems. Example 5 shows the terms in the general equation expanded so that they might serve as a quick reference for other problems. The problem deals with a six-winding transformer.

Basic relations are used in the analysis:

(1) $N_1I_1 - N_2I_2 = O$ (2) $V_1 - V_2 = IZ_{SC}$

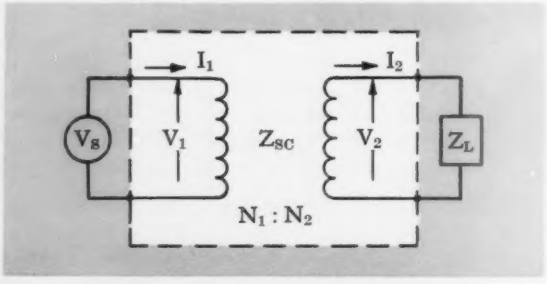

Simple two-winding transformer is origin of general relations for more complex circuitry.

Equation 1 states that ampere turns add up to zero. This equation ignores excitation

Equation 2 states that voltage difference at transformer terminals is equal to the leakage impedance drop through the transformer.

(3) $V_1 = V_S$ (4) $I_2Z_L = V_2$

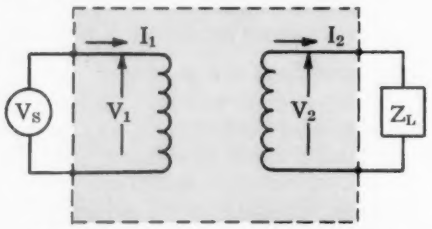

External circuit furnishes the additional equations required to solve for the unknown.

General expressions for equations 1 and 2 are as follows;

$$I_1 + \sum_{k=n}^{k=2} (n_kI_k) = 0$$

$$(V_j/n_j - V_1) = \sum_{k=2}^{k=n} \frac{1}{2}(Z_{1-j} + Z_{1-k} - Z_{j-k})(n_kI_k);$$

$$j = 2 \text{ - - - - } n$$

where "j" is the number of the winding for which the equation is written, and "n" represents the number of magnetically coupled windings in the particular portion of the circuit for which the equation is written.

Also $n_k = \left(\frac{N_k}{N_1}\right)$.

The following should be noted in the general expressions of 1 and 2;

1. The Z_{1-j}, Z_{1-k}, and Z_{j-k} terms are the leakage or nameplate impedances.
2. Since V_j/n_j is the voltage of the "jth" winding referred to the 1 winding and $\sum_{k=2}^{n} n_kI_k$ are the currents referred to the 1 winding, the leakage impedances must also be referred to the 1 winding.
3. The rules for signs in the general equations 1 and 2 are "K" windings having loads are $-n_kI_k$ and "K" windings having sources are $+n_kI_k$. I_1 obeys the same rules. These rules are used for less complex problems.
4. The load impedances such as "Z_L" in equation 4 are not referred to the 1 winding.
5. "N" windings result in "N" transformer equations and "N" external circuit equations. These equations are used to solve for the "2N" unknowns.
6. The general equations are the origin of many of the equivalent circuits used today in system analysis.

Examples illustrate equation application

EXAMPLE 1 — Illustrates the use of the equations in their simplest form; the results can be checked by simple circuit theory.

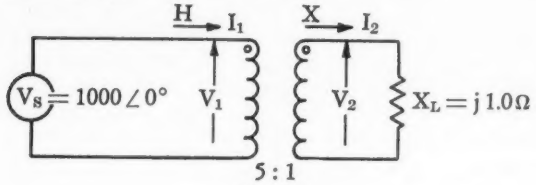

$$n_2 = \frac{N_2}{N_1} = \frac{1}{5} = .2$$

10 KVA $5\% = Z_t = Z_{1-2}$

$V_{b1} = 1000$ $\qquad$ $V_{b2} = 200$

$$I_{b1} = \frac{10000}{1000} = 10 \qquad I_{b2} = \frac{10000}{200} = 50$$

$$Z_{b1} = \frac{1000}{10} = 100 \qquad Z_{b2} = \frac{200}{50} = 4$$

$X_{tH}\Omega = (P_u)(Z_{b1}) = .05 \times 100 = j\,5\Omega = Z_{1-2}$

$X_{tX}\Omega = (P_u)(Z_{b2}) = .05 \times 4 = j\,.2\Omega = Z_{1-2}$

$$P_u X_L = \frac{a}{b} = \frac{j\,1.0}{4} = j\,.25$$

General equations

$$I_1 + \sum_{k=2}^{2} n_k I_k = 0$$

$$(V_j/n_j - V_1) = \sum_{k=2}^{2} \frac{1}{2}(Z_{1-j} + Z_{1-k} - Z_{j-k})(n_k I_k)$$

$j = 2 \cdots (n = 2)$

OHM METHOD

(1) $I_1 - .2I_2 = 0$

(2) $V_2/.2 - V_1 = \frac{1}{2}(Z_{1-2} + Z_{1-2} - Z_{2-2})(-.2)\,I_2$

$= (j\,5.0)(-0.2)I_2$ where $Z_{2-2} = 0$

(3) $V_1 = 1000\angle 0°$

(4) $V_2 = I_2 X_L = j\,1.0 I_2$

Substituting (3) and (4) into (2) yields:

$j\,6I_2 = 1000\angle 0°$

$$I_2 = \frac{1000\angle 0°}{j\,6.0} = 166.7\angle -90°$$

$I_1 = .2I_2 = .2(166.7\angle -90°) = 33.3\angle -90°$

$V_2 = j\,1.0(166.7\angle -90°) = 166.7\angle 0°$

P_u METHOD

(1) $I_1 - I_2 = 0$

(2) $V_2 - V_1 = (j.05)(-I_2)$

(3) $V_1 = 1.0\angle 0°$

(4) $V_2 = I_2(j.25)$

Substituting (3) and (4) into (2) yields:

$j.3I_2 = 1.0\angle 0°$

$$I_2 = \frac{1.0}{j.3} = 3.33\angle -90°$$

$= 3.33\angle -90° \times 50 = 166.5\angle -90°$ amperes.

$I_1 = I_2 = 3.33\angle -90°$

$= 3.33\angle -90° \times 10 = 33.3\angle -90°$ amperes.

$V_2 = 3.33(.25) = .832\angle 0°$

$= .832\angle 0° \times 200 = 166.4\angle 0°$ volts.

The parallel development of the ohmic and the per unit methods shows how the equations work equally well for the simple cases. The "n" terms (turns ratios) drop out of the equation in the per unit method.

An additional illustration aids in properly interpreting the signs in the general equations. Consider the same circuit but with the windings numbered in reverse, (1) becomes (2) and (2) becomes (1). The results agree.

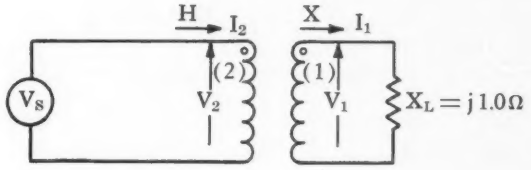

$Z_{1-2} = j.2\Omega$ $\qquad$ $n_2 = \frac{N_2}{N_1} = 5$

(1) $-I_1 + 5I_2 = 0$

(2) $\frac{V_2}{5} - V_1 = j.2(+5I_2)$

(3) $V_2 = 1000\angle 0°$

(4) $V_1 = I_1 X_L = j\,1.0 I_1$

Substituting (3) and (4) into (2) which is then solved in conjunction with (1) multiplied through by $+j$

$200\angle 0° = j\,1.0I_1 + j\,1.0I_2$

$0 = -I_1 + 5I_2$

$200\angle 0° = j6.0I_2$

$$I_2 = \frac{200\angle 0°}{j6.0} = 33.3\angle -90°$$

$I_1 = 5I_2 = 166.5\angle -90°$

$V_1 = j\,1.0(166.5\angle -90°) = 166.5\angle 0°$

In general, where currents are indicated as entering the polarity mark of the winding, the signs in the equations for the currents are plus. This approach is used in the more complex circuits. The relation between signs in the equation and current direction is shown by Example 1.

EXAMPLE 2 — Illustrates the use of the equations when windings are connected to form an autotransformer. It should be noted that the equations for the autotransformer connection were as easily written as for the conventional two-winding transformer in Example 1.

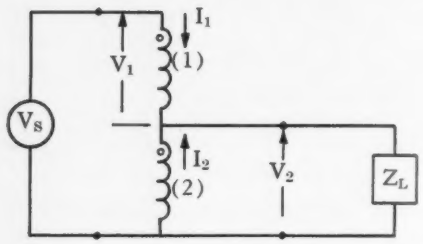

Given:

$Z_{1-2} = j1.0\Omega_1$

$Z_L = j1.0\Omega$

$N_1/N_2 = 1/5$

$V_S = 138\angle 0°$

Find I_1, I_2, V_1 and V_2

TRANSFORMER EQUATIONS

(1) $I_1 - n_2 I_2 = 0$

(2) $\dfrac{V_2}{n_2} - V_1 = \dfrac{1}{2}(Z_{1-2} + Z_{1-2} - Z_{2-2})(-n_2 I_2)$

$(Z_{2-2} = 0)$

CIRCUIT EQUATIONS

(3) $V_1 + V_2 = V_S$

(4) $(I_1 + I_2)\, Z_L = V_2$

since:

$$n_2 = \frac{N_2}{N_1} = \frac{5}{1} = 5 \; ; \; V_S = 138\angle 0°$$

$$Z_{1-2} = j1.0 \; ; \; Z_L = j1.0$$

we can write equations 1 to 4 as follows;

(1) $I_1 - 5I_2 = 0$

(2) $.2V_2 - V_1 = (-j5I_2)$

(3) $V_1 + V_2 = 138\angle 0°$

(4) $(I_1 + I_2)(j1) = V_2$

Solving for the unknowns:

	I_1	I_2	V_1	V_2	
(1)	I_1	$-5I_2$	$+0$	$+0$	$=0$
(2)	0	$+j5I_2$	$-V_1$	$+.2V_2$	$=0$
(3)	0	$+0$	$+V_1$	$+V_2$	$=138\angle 0°$
(4)	jI_1	$+jI_2$	$+0$	$-V_2$	$=0$

Multiplying (1) by $-j$ and adding to (4) yields (a)

(a) $j6I_2 + 0 - V_2 = 0$

Multiplying (2) by 6/5 and adding to (a) yields (b)

(b) $+1.2V_1 - 1.24V_2 = 0$

$$V_1 = \frac{1.24}{1.2} V_2 = 1.033V_2$$

Substituting into equation (3)

$1.033V_2 + V_2 = 138\angle 0°$

$$V_2 = \frac{138\angle 0°}{2.033} = 67.9\angle 0°$$

$$V_1 = 1.033(67.9\angle 0°) = 70\angle 0°$$

$$I_2 = \frac{V_2}{j6} = \frac{67.9\angle 0°}{j6} = 11.3\angle -90°$$

$$I_1 = 5I_2 = 5(11.3\angle -90°) = 56.5\angle -90°$$

EXAMPLE 3 — The danger of an ungrounded autotransformer is brought out using the general equations in this example. Voltage inversion occurs raising the neutral point of the transformer to a voltage greater than line-to-line system voltage.

Solving this problem by conventional ac circuit theory using self and mutual impedances is a task, and the use of symmetrical components to such a circuit appears to be impossible. A solution by the general equations follows:

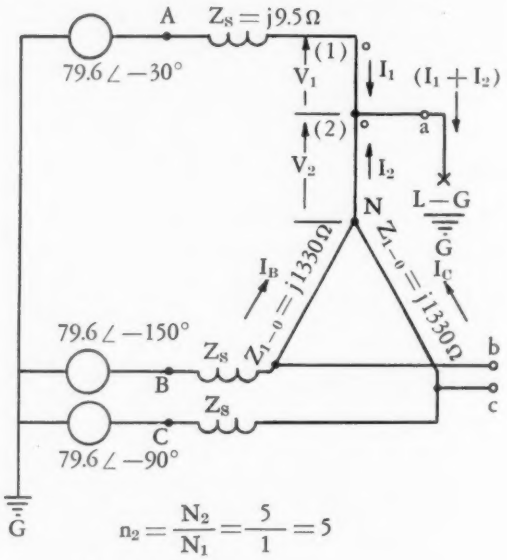

$$n_2 = \frac{N_2}{N_1} = \frac{5}{1} = 5$$

$KVA_T = 50\,MVA$

$$Z_b = \frac{(138)^2 K^2}{50\,M} = 380$$

$Z_{1-2} = j.0167 \times 380 = j6.35\Omega$

$Z_{1-0} = j3.5 \times 380 = 1330\Omega$

$Z_S = .025 \times 380 = 9.5\Omega$

where transformer impedances were measured as follows:

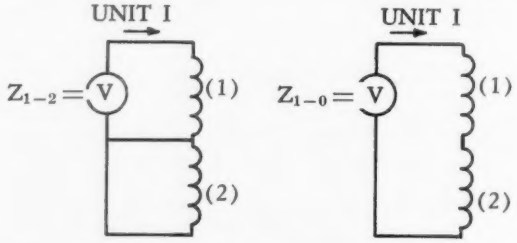

(1) $I_1 - n_2 I_2 = 0 \; ; \; I_1 - 5I_2 = 0$

(2) $\dfrac{V_2}{n_2} - V_1 = (Z_{1-2})(-n_2 I_2)$;

$.2V_2 - V_1 = j6.35(-5)I_2 = j(-j31.7)I_2$

Since I_B and I_C are unknown, 4 circuit equations must be established instead of the normal 2.

(3) $I_B + I_C = I_2$

(4) $I_1(j9.5) + V_1 = 79.6K \angle -30°$

(5) $I_B(j1339) - V_2 = 79.6K \angle -150°$

(6) $I_C(j1339) - V_2 = 79.6K \angle 90°$

Adding (5)+(6) then substituting (3) into (5)+(6) yields:

(7) $I_2(j1339) - 2V_2 = 79.6K \angle 150°$

Equations (1), (2), (4) and (7) can be solved as follows:

	I_1	I_2	V_1	V_2	
(1)	I_1	$-5I_2$	$+0$	$+0$	$=0$
(2)	0	$+j31.7I_2$	$-V_1$	$+.2V_2$	$=0$
(4)	$j9.5I_1$	$+0$	$+V_1$	$+0$	$=79.6K \angle -30°$
(7)	0	$+j1339I_2$	$+0$	$-2V_2$	$=76.6K \angle 150°$

Multiplying (2) by 10 and adding to (7) yields (a).

(a) $j1656I_2 - 10V_1 = 79.6K \angle 150°$

Multiplying (1) by (j1656/5) and adding to (a) yields (b).

(b) $j331I_1 - 10V_1 = 79.6K \angle 150°$

Multiplying (4) by 10 and adding to (b) yields (c).

(c) $j426I_1 = (79.6K \angle -30° + 79.6K \angle 150°)$

$$I_1 = \frac{717K}{.426K} \angle -120° = 1.68K \angle -120°$$

$$I_2 = \frac{I_1}{5} = \frac{1.68K}{5} = .336K \angle -120°$$

$$I_1 + I_2 = 2.02K \angle -120°$$

$$V_2 = \frac{j1.339K\,(.336K) \angle -120° + 79.6K \angle -30°}{2}$$

$$= \frac{529K}{2} \angle -30° = 264KV \angle -30°$$

$$V_1 = 79.6K \angle -30° - (j9.5)(1.68K \angle -120°)$$

$$= 63.6\ KV \angle -30°$$

---

(3) $I_B + I_C = .336K \angle -120°$

(5)−(6) $I_B(j1.339K) - I_C(j1.339K) = (79.6K \angle -150° - 79.6K \angle 90°)$

$$j2.68KI_B = (450K \angle -30° + 138K \angle -120°)$$

$$I_B = \frac{470K \angle -47°}{2.68K \angle 90°} = 175 \angle -137°$$

$$I_C = (.336K \angle -120° - 175 \angle -137°)$$

$$= 175 \angle -103°$$

Voltage inversion results from the current being forced through the "B" and "C" windings. The "B" and "C" phase windings have no canceling mmf and the high reactance forces the neutral voltage well above line-to-line voltage.

EXAMPLE 4 — A slightly different type of problem is solved by the use of the general equations. At times it is necessary to determine equivalent impedances of transformers that have multi-windings which can be connected in various ways. A three-winding transformer will be used as an illustration:

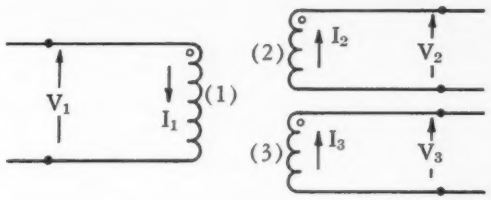

$$I_1 + \sum_{k=2}^{n} n_k I_k = 0$$

$$(V_j/n_j - V_1) = \sum_{k=2}^{3} \frac{1}{2}(Z_{1-j} + Z_{1-k} - Z_{1-k})\, n_k I_k$$

$$j = 2 \cdots 3$$

$Z_{1-2} = .092$
$Z_{1-3} = .124$
$Z_{2-3} = .048$
} Impedances in per unit on a common KVA base.

a. Series connection of (2) and (3).

(1) $I_1 - I_2 - I_3 = 0$

(2) $(V_2 - V_1) = Z_{1-2}(-I_2) + \left(\frac{Z_{1-2} + Z_{1-3} - Z_{2-3}}{2}\right)(-I_3)$

where $\frac{Z_{1-2} + Z_{1-3} - Z_{2-3}}{2} = .084$

(3) $(V_3 - V_1) = \left(\frac{Z_{1-3} + Z_{1-2} - Z_{3-2}}{2}\right)(-I_2) + Z_{1-3}(-I_3)$

(4) $I_1 = 1$; Passing unit of current makes $V_1 = Z_{1-23\ equiv.}$ by definition.

(5) $I_2 = I_3$

(6) $V_2 + V_3 = 0$

Adding (2)+(3) yields:

$$-(V_2 + V_3) + 2V_1 = .176I_2 + .208I_3$$

Since $I_2 = I_3$ we can say: $I_1 = 2I_2$ or $I_2 = .5$

Also: $2V_1 = .384I_2 = .384\,(.5) = .192$

Therefore $V_1 = \frac{.192}{2} = .091 = Z_{1-23\ equiv.}$

b. Parallel connection of (2) and (3).

(1) $I_1 - I_2 - I_3 = 0$

(2) $V_2 - V_1 = Z_{1-2}(-I_2) + \left(\frac{Z_{1-2} + Z_{1-3} - Z_{2-3}}{2}\right)(-I_3)$

(3) $V_3 - V_1 = \left(\frac{Z_{1-3} + Z_{1-2} - Z_{3-2}}{2}\right)(-I_2) + Z_{1-3}(-I_3)$

(4) $V_2 = 0$

(5) $I_1 = 1$

(6) $V_3 = 0$

---

(2) $-V_1 = -.092I_2 - .084I_3$

(3) $V_1 - .084I_2 + .124I_3$

Adding (2)+(3) yields (a).

(a) $0 = -.008I_2 + .04I_3$
from (1) and (5)

(b) $1 = I_2 + I_3$

Multiplying (b) by $-.04$ and adding to (a) yields

$$-.048I_2 = .04$$

$$I_2 = \frac{.04}{.048} = .833$$

$$I_3 = (1 - I_2) = .167$$

$$V_1 = .084\,(.833) + .124\,(.167) = .0907 = Z_{1-23\ \text{equiv.}}$$

EXAMPLE 5 — The general equations are valid for any number of windings. Consider the six-winding transformer shown below as an illustration of the analysis involved.

$Z_{1-2} = j.1$
$Z_{1-3} = j.2$
$Z_{1-4} = j.3$
$Z_{1-5} = j.1$
$Z_{1-6} = j.2$
$Z_{2-3} = j.1$
$Z_{2-4} = j.2$
$Z_{2-5} = j.3$
$Z_{2-6} = j.4$
$Z_{3-4} = j.1$
$Z_{3-5} = j.2$
$Z_{3-6} = j.3$
$Z_{4-5} = j.1$
$Z_{4-6} = j.2$
$Z_{5-6} = j.1$

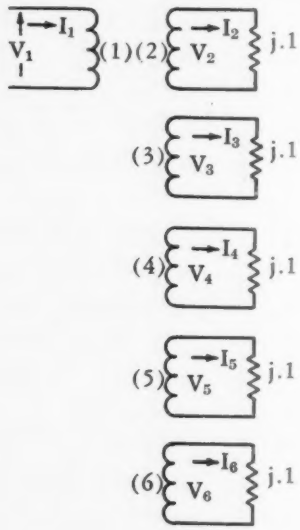

$V_1 = 100 \angle 0°$

$n_1 = n_2 = n_3 = n_4 = n_5 = n_6 = 1$

$$I_1 + \sum_{k=2}^{6} n_k j_k = 0$$

$$\left(\frac{V_j}{n_j} - V_1\right) = \sum_{k=2}^{6} \frac{1}{2}(Z'_{jk})\,(n_k I_k)$$

The first six equations are developed from the general equations. These transformer equations shown expanded with general terms can be used as a reference for other problems.

REFERENCE EQUATIONS

1 $I_1 - n_2I_2 - n_3I_3 - n_4I_4 - n_5I_5 - n_6I_6 = 0$

2 $$\left(\frac{V_2}{n_2} - V_1\right) = \frac{1}{2}\Big[(Z_{1-2} + Z_{1-2} - Z_{2-2})(-n_2I_2)\Big] + \frac{1}{2}\Big[(Z_{1-2} + Z_{1-3} - Z_{2-3})(-n_3I_3)\Big] + \frac{1}{2}\Big[(Z_{1-2} + Z_{1-4} - Z_{2-4})(-n_4I_4)\Big] + \frac{1}{2}\Big[(Z_{1-2} + Z_{1-5} - Z_{2-5})(-n_5I_5)\Big] + \frac{1}{2}\Big[(Z_{1-2} + Z_{1-6} - Z_{2-6})(-n_6I_6)\Big]$$

3 $$(V_3 - V_1) = \frac{1}{2}\Big[(Z_{1-3} + Z_{1-2} - Z_{3-2})(-I_2)\Big] + \frac{1}{2}\Big[(Z_{1-3} + Z_{1-3} - Z_{3-3})(-I_3)\Big] + \frac{1}{2}\Big[(Z_{1-3} + Z_{1-4} - Z_{3-4})(-I_4)\Big] + \frac{1}{2}\Big[(Z_{1-3} + Z_{1-5} - Z_{3-5})(-I_5)\Big] + \frac{1}{2}\Big[(Z_{1-3} + Z_{1-6} - Z_{3-6})(-I_6)\Big]$$

4 $$(V_4 - V_1) = \frac{1}{2}\Big[(Z_{1-4} + Z_{1-2} - Z_{4-2})(-I_2)\Big] + \frac{1}{2}\Big[(Z_{1-4} + Z_{1-3} - Z_{4-3})(-I_3) + \frac{1}{2}\Big[(Z_{1-4} + Z_{1-4} - Z_{4-4})(-I_4)\Big] + \frac{1}{2}\Big[(Z_{1-4} + Z_{1-5} - Z_{4-5})(-I_5)\Big] + \frac{1}{2}\Big[(Z_{1-4} + Z_{1-6} - Z_{4-6})(-I_6)\Big]$$

5 $$(V_5 - V_1) = \frac{1}{2}\Big[(Z_{1-5} + Z_{1-2} - Z_{5-2})(-I_2)\Big] + \frac{1}{2}\Big[(Z_{1-5} + Z_{1-3} - Z_{5-3})(-I_3)\Big] + \frac{1}{2}\Big[(Z_{1-5} + Z_{1-4} - Z_{5-4})(-I_4)\Big] + \frac{1}{2}\Big[(Z_{1-5} + Z_{1-5} - Z_{5-5})(-I_5)\Big] + \frac{1}{2}\Big[(Z_{1-5} + Z_{1-6} - Z_{5-6})(-I_6)\Big]$$

6 $$(V_6 - V_1) = \frac{1}{2}\Big[(Z_{1-6} + Z_{1-2} - Z_{6-2})(-I_2)\Big] + \frac{1}{2}\Big[(Z_{1-6} + Z_{1-3} - Z_{6-3})(-I_3)\Big] + \frac{1}{2}\Big[(Z_{1-6} + Z_{1-4} - Z_{6-4})(-I_4)\Big] + \frac{1}{2}\Big[(Z_{1-6} + Z_{1-5} - Z_{6-5})(-I_5)\Big] + \frac{1}{2}\Big[(Z_{1-6} + Z_{1-6} - Z_{6-6})(-I_6)\Big]$$

Note: $Z_{2-2}, Z_{3-3}, Z_{4-4}, Z_{5-5}$, and Z_{6-6} all equal zero. Since the turns ratios in Example 5 were equal to 1, the "n_k" terms were omitted in equations (3) to (6). Equations (1) and (2) contain the "n_k" terms.

The three leakage (short circuit) impedances in each bracket represent the equivalent branch impedances commonly used in representing three-winding transformers. The whole equation made up of five such terms is based on the principle of five superpositions of five such *T* circuits.

The circuit equations follow:

(7) $V_1 = 100 \angle 0°$

(8) $V_2 = j.1I_2$

(9) $V_3 = j.1I_3$

(10) $V_4 = j.1I_4$

(11) $V_5 = j.1I_5$

(12) $V_6 = j.1I_6$

After equation (7) through (12) are substituted in equation (2) through (6) and numerical values are substituted into equation (1) through (6), the following equation can be established and reduced by matrix algebra.

The six unknown currents are obtained from the matrix reduction.

$$I_6 = \frac{25 \angle 0°}{j.2} = 125 \angle -90°$$

$$I_5 = \frac{25}{j.1} = 250 \angle -90°$$

$$I_4 = \left(\frac{20 \angle 0° - j.13\,(250 \angle -90°) - j.13\,(125 \angle -90°)}{j.26} \right)$$

$$= \frac{-28.75 \angle 0°}{j.26} = 110.5 \angle 90°$$

$$I_3 = \left(\frac{50 \angle 0° - j.15\,(110.5 \angle 90°) - j.075\,(375 \angle -90°)}{j.25} \right)$$

$$= \frac{38.5 \angle 0°}{j.25} = 154 \angle -90°$$

$$I_2 = \frac{100 \angle 0° + j.1\,(43.5 \angle -90°) - j.05\,(375 \angle -90°)}{j.2}$$

$$= \frac{85.6 \angle 0°}{j.2} = 428 \angle -90°$$

$$I_1 = (428 \angle -90° + 154 \angle -90° + 250 \angle -90° + 125 \angle -90° - 110.5 \angle -90°) = 846.5 \angle -90°$$

While the examples show but a few applications of the general equations, knowledge of how they are applied will help with a number of other types of problems encountered in system studies. A line-to-ground fault study on a system having autotransformers and requiring close relay settings is such a problem.

It is well to take a second look before assuming some transformer circuit problems are too difficult to solve. The general equations may provide the answers.

REFERENCES

1. *Introductory Circuit Theory*, E. A. Guillemin, John Wiley & Sons, New York, 1953.
2. *Alternating Current Machinery*, L. V. Bewley, The Macmillan Co., New York, 1949.

MATRIX REDUCTION OF SIMULTANEOUS EQUATIONS

	I_1	I_2	I_3	I_4	I_5	I_6	
(1)	I_1	$-I_2$	$-I_3$	$-I_4$	$-I_5$	$-I_6$	$=0$
(2)	0	$+j.2I_2$	$+j.1I_3$	$+j.1I_4$	$-j.05I_5$	$-j.05I_6$	$=100 \angle 0°$
(3)	0	$+j.1I_2$	$+j.3I_3$	$+j.2I_4$	$+j.05I_5$	$+j.05I_6$	$=100 \angle 0°$
(4)	0	$+j.1I_2$	$+j.2I_3$	$+j.4I_4$	$+j.15I_5$	$+j.15I_6$	$=100 \angle 0°$
(5)	0	$-j.05I_2$	$+j.05I_3$	$+j.15I_4$	$+j.2I_5$	$+j.1I_6$	$=100 \angle 0°$
(6)	0	$-j.05I_2$	$+j.05I_3$	$+j.15I_4$	$+j.1I_5$	$+j.3I_6$	$=100 \angle 0°$
(3)′			$+j.25I_3$	$+j.15I_4$	$+j.075I_5$	$+j.075I_6$	$=50 \angle 0°$
(4)′			$+j.15I_3$	$+j.35I_4$	$+j.175I_5$	$+j.175I_6$	$=50 \angle 0°$
(5)′			$+j.075I_3$	$+j.175I_4$	$+j.1875I_5$	$+j.0875I_6$	$=75 \angle 0°$
(6)′			$+j.075I_3$	$+j.175I_4$	$+j.0875I_5$	$+j.2875I_6$	$=75 \angle 0°$
(4)″				$+j.26I_4$	$+j.13I_5$	$+j.13I_6$	$=20 \angle 0°$
(5)″				$+j.13I_4$	$+j.165I_5$	$+j.065I_6$	$=35 \angle 0°$
(6)″				$+j.13I_4$	$+j.065I_5$	$+j.265I_6$	$=35 \angle 0°$
(5)‴					$+j.1I_5$	$+0$	$=25 \angle 0°$
(6)‴					0	$+j.2I_6$	$=25 \angle 0°$

Research and Development

Provide Data for Advanced Nuclear Power Plant

Important steps are being made in the development of plants that can provide more economical nuclear power.

Information gained from the test loop shown is being used to finalize designs of the Controlled Recirculation Boiling Reactor for the Pathfinder Atomic Power Plant. High velocity water circulated through the Pathfinder reactor will rapidly move steam from the core. The design will provide a considerable gain in power per unit of reactor volume over earlier boiling-water reactors. Reactor power output will be controlled by varying the coolant flow rate through the reactor core.

Flow conditions in the test sections are dynamically similar to those of the Pathfinder Plant. The test loop was designed to obtain data for important reactor components. The loop includes a prototype of the centrifugal steam separator that will be used in the reactor downcomer section. A model of the valves used to control pump output is also part of the test loop.

The copper tubing connected to the vertical test section provides a means of determining densities of the water-steam mixture above the reactor core. This information will be used for calibration of liquid-level instruments on the Pathfinder reactor.

Experience gained in building and testing nuclear power plant components is expected to point the way to lower-cost nuclear power.

by **DAVID H. SWANSON**
Nuclear Power Department — Greendale
Allis-Chalmers Manufacturing Company